Lithos 112 (2009) 1–17

Contents lists available at ScienceDirect

Lithos

journal homepage: www.elsevier.com/locate/lithos

MORB mantle hosts the missing Eu (Sr, Nb, Ta and Ti) in the continental crust: New perspectives on crustal growth, crust–mantle differentiation and chemical structure of oceanic upper mantle

Yaoling Niu [a,*], Michael J. O'Hara [b]

[a] Department of Earth Sciences, Durham University, Durham DH1 3LE, UK
[b] Institute of Geography and Earth Sciences, Aberystwyth University, Aberystwyth SY23 3DB, UK

ARTICLE INFO

Article history:
Received 28 May 2008
Accepted 10 December 2008
Available online 24 December 2008

Keywords:
Eu, Sr, Nb, Ta and Ti anomalies
Plagioclase
Amphibolite
Primitive MORB
Low velocity zone dynamics
Oceanic upper mantle compositional structure
Crust–mantle differentiation
Continental crust growth

ABSTRACT

We have examined the high quality data of 306 mid-ocean ridge basalt (MORB) glass samples from the East Pacific Rise (EPR), near-EPR seamounts, Pacific Antarctic Ridge (PAR), near-PAR seamounts, Mid-Atlantic Ridge (MAR), and near-MAR seamounts. The data show a correlated variation between Eu/Eu* and Sr/Sr*, and both decrease with decreasing MgO, pointing to the effect of plagioclase crystallization. The observation that samples with MgO>9.5 wt.% (before plagioclase on the liquidus) show Eu/Eu*>1 and Sr/Sr*>1 and that none of the major phases (i.e., olivine, orthopyroxene, clinopyroxene, spinel and garnet) in the sub-ridge mantle melting region can effectively fractionate Eu and Sr from otherwise similarly incompatible elements indicates that the depleted MORB mantle (DMM) possesses excess Sr and Eu, i.e., $[Sr/Sr^*]^{DMM}>1$ and $[Eu/Eu^*]^{DMM}>1$. Furthermore, the well-established observation that $D^{Nb}\approx D^{Th}$, $D^{Ta}\approx D^{U}$ and $D^{Ti}\approx D^{Sm}$ during MORB mantle melting, yet primitive MORB melts all have $[Nb/Th]_{PM}^{MORB}>1$, $[Ta/U]_{PM}^{MORB}>1$ and $[Ti/Sm]_{PM}^{MORB}>1$ (where $_{PM}$ indicates primitive mantle normalized), also points to the presence of excess Nb, Ta and Ti in the DMM, i.e., $[Nb/Th]_{PM}^{DMM}>1$, $[Ta/U]_{PM}^{DMM}>1$ and $[Ti/Sm]_{PM}^{DMM}>1$. The excesses of Eu, Sr, Nb, Ta and Ti in the DMM complement the well-known deficiencies of these elements in the bulk continental crust (BCC). These new observations, which support the notion that the DMM and BCC are complementary in terms of the overall abundances of incompatible elements, offer new insights into the crust–mantle differentiation. These observations are best explained by partial melting of amphibolite of MORB protolith during continental collision, which produces andesitic melts with a remarkable compositional (major and trace element abundances as well as key elemental ratios) similarity to the BCC, as revealed by andesites in southern Tibet produced during the India–Asia continental collision. An average amphibolite of MORB protolith consists of ~66.4% amphibole, ~29.2% plagioclase and 4.4% ilmenite. In terms of simple modal melting models, the bulk distribution coefficient ratios $D^{2Eu/(Sm+Gd)}=1.21$, $D^{2Sr/(Pr+Nd)}=1.04$, $D^{Nb/Th}=44$, $D^{Ta/U}=57$, $D^{Ti/Sm}=3.39$ and $D^{Nb/Ta}=1.30$ readily explains the small but significant negative Eu and Sr anomalies, moderate negative Ti anomaly and huge negative Nb and Ta anomalies as well as the more sub-chondritic Nb/Ta ratio in the syncollisional andesitic melt that is characteristic of and contributes to the continental crust mass. These results support the hypothesis that continental collision zones are primary sites of net continental crust growth, whereas the standard "island arc" model has many more difficulties than certainties. That is, it is the continental collision (vs. "island arc magmatism" or "episodic super mantle avalanche events") that produces and preserves the juvenile crust, and hence maintains net continental growth. The data also allow us to establish the robust composition of depleted and most primitive (or "primary") MORB melt with 13% MgO. This, together with the estimated positive Eu and Sr anomalies in the DMM, further permits estimation that the DMM may occupy the uppermost ~680 km of the convective mantle following the tradition that the DMM lies in the shallowest mantle. However, the tradition may be in error. The seismic low velocity zone (LVZ) may be compositionally stratified with small melt fractions concentrated towards the interface with the growing lithosphere because of buoyancy. Such small melt fractions, enriched in volatiles and incompatible elements, continue to metasomatize the growing lithosphere before it reaches the full thickness after ~70 Myrs. Hence, the oceanic mantle lithosphere is a huge enriched geochemical reservoir. On the other hand, deep portions of the LVZ, which are thus relatively depleted, become the primary source feeding the ridge because of ridge-suction-driven lateral material supply to form the crust and much of the lithosphere at and in the vicinity of the ridge.

* Corresponding author.
E-mail address: Yaoling.Niu@durham.ac.uk (Y. Niu).

0024-4937/$ – see front matter © 2008 Elsevier B.V. All rights reserved.
doi:10.1016/j.lithos.2008.12.009

The important thing in science is not so much to obtain new facts as to discover new ways of thinking about them. — Sir William Bragg.

1. Introduction

The incompatible element depleted nature of mid-ocean ridge basalts (MORB) is widely accepted as reflecting their depleted mantle source. Because ocean ridges are mostly passive features in the sense that the sub-ridge mantle rises and melts by decompression in response to plate separation, it follows that MORB sample the uppermost asthenospheric mantle. As a result, the oceanic upper mantle has been designated as depleted MORB mantle (DMM) (Zindler and Hart, 1986), whose origin is generally thought to have resulted from continental crust extraction in Earth's early history (e.g., Gast, 1968; O'Nions et al., 1979; Allègre et al., 1983). This inference is supported by the first order complementarity in terms of incompatible element abundances between average continental crust and oceanic crust approximated by average MORB (Hofmann, 1988). Hofmann (1988) further suggested that extraction of a small amount of very low-degree (~1.5% melting) melt from the primitive mantle produced the incompatible-element-enriched continental crust in Earth's early history, and left behind an incompatible-element-depleted residue (i.e., DMM) in the upper mantle that became the source of MORB. The mean age of the continental crust is ~2.0–2.5 Ga (e.g., Jacobsen and Wasserburg, 1979; Taylor and McLennan, 1985), implying a similar mean age for the DMM.

While "island arc" model (Taylor, 1967, 1977) has been widely accepted as the primary mechanism through which mantle derived melts contribute to continental crust mass, the actual physical and chemical processes involved remain elusive (e.g., Rudnick and Gao, 2003; Kelemen et al., 2003a,b; Plank, 2005; Hawkesworth and Kemp, 2006; Davidson and Arculus, 2006; Niu et al., 2007; Mo et al., 2008). In this paper, we re-examine high quality MORB data and show that primitive MORB melts have excess Eu (or a positive Eu anomaly with respect to its adjacent rare earth elements Sm and Gd). This excess Eu is inherited from the DMM source, which complements the missing Eu (or a negative Eu anomaly) in the bulk continental crust (Rudnick and Gao, 2003). The similar behaviour of Sr to that of Eu explicitly points to the role of plagioclase in the growth of continental crust from mantle derived melts. We also show that melting of amphibolite of MORB protolith during continental collision explains the observed crust–mantle distribution of Eu and Sr, enrichments of progressively more incompatible elements, Nb–Ta–Ti depletion and the more sub-chondritic Nb/Ta ratio characteristic of continental crust without invoking active subduction-zone magmatism, which, among other difficulties, produces variably high excess Sr that is inconsistent with the chemical property of the continental crust that has, if anything, a weak Sr deficiency.

2. Excess Eu and Sr in primitive MORB

2.1. Rare earth elements and petrogenesis

Modern theories of petrogenesis owe much to the ability to analyze rare earth elements (REEs) in rocks and their applications (e.g., Frey et al., 1968; Hanson, 1980). The power of REEs lies in the fact that under geological conditions all the naturally occurring 14 of these elements, except for Eu and Ce, are trivalent (i.e., R^{3+}), and have ionic radii that increase systematically from the heaviest Lu (Z = 71) to the lightest La (Z = 57) for a given coordination in crystal structures, leading to systematic change in relative incompatibilities (or mineral/melt partition coefficients) as a function of atomic number (Z). Therefore, on chondrite or primitive mantle normalized diagrams, REE patterns of natural rocks are smooth, but their varying abundance levels and topologies, in the case of silicate melts for example, carry messages about the mineralogy, chemistry and histories of source rocks, the extent (and pressure) of melting, crystallization, mixing, assimilation etc. The Ce and Eu may behave in "unusual" ways, which can in fact offer additional insights. Under oxidizing conditions at and near Earth's surface, Ce can be partially oxidized to Ce^{4+}, which is much smaller ($r^{Ce^{4+}}_{CN=6} = 0.861$ Å vs. $r^{Ce^{3+}}_{CN=6} = 1.01$ Å) (Shannon, 1976), and can readily fractionate from its neighbouring La ($r^{La^{3+}}_{CN=6} = 1.032$) and Pr ($r^{Pr^{3+}}_{CN=6} = 0.99$) (e.g., seen in rivers, sediments, soils and seafloor Mn precipitates), but in most magmatic rocks Ce maintains its trivalent state. On the other hand, under reduced conditions, Eu can be partially reduced to Eu^{2+} that is much larger ($r^{Eu^{2+}}_{CN=6} = 1.17$ vs. $r^{Eu^{3+}}_{CN=6} = 0.947$), and can thus readily fractionate from its neighbouring Sm ($r^{Sm^{3+}}_{CN=6} = 0.958$) and Gd ($r^{Gd^{3+}}_{CN=6} = 0.938$), causing the familiar concept of Eu anomaly in rocks. The Eu reduction may not necessarily take place in the last petrogenetic event, and the reduced Eu^{2+} present in rocks of interest is mostly inherited from previous processes and source histories. Note that the divalent Sr^{2+} behaves very similarly to Eu^{2+} because of their very similar ionic radii (i.e., $r^{Eu^{2+}}_{CN=6} = 1.17 \approx r^{Sr^{2+}}_{CN=6} = 1.18$). Therefore, rocks with Eu anomalies that show correlated variations with Sr must result from a common process or processes. We show below that it is the anomalous Eu in MORB melts and its co-variation with Sr along with Nb, Ta and Ti "anomalies" that lead to our new perspectives on important aspects of crust–mantle differentiation and continental crust growth.

2.2. Common perception: no Eu anomaly in mantle derived melts

Fig. 1 shows that on chondrite-normalized REE diagram, average compositions of mantle derived melts such as ocean island basalts (OIB), normal mid-ocean ridge basalts (N-MORB), enriched-type MORB (E-MORB) and island arc basalts (IAB) all show smooth REE patterns with no Eu anomalies. If the DMM as reflected by average MORB is indeed complementary to the continental crust (Hofmann, 1988), then there should be no Eu anomaly in the bulk continental crust (BCC) because the primitive mantle (PM, the same as bulk silicate Earth, BSE), from which the BCC and DMM are assumed to have derived, has constant REE values ~2.9 times the chondrite REE abundances without a Eu anomaly (Fig. 1). However, this is not the case (see below). Note that our discussion is based on the common assumption that the bulk earth is of chondritic composition with the exception of some volatile elements, and the BSE or PM possess all the non-siderophile/chalcophile elements of bulk earth after core separation.

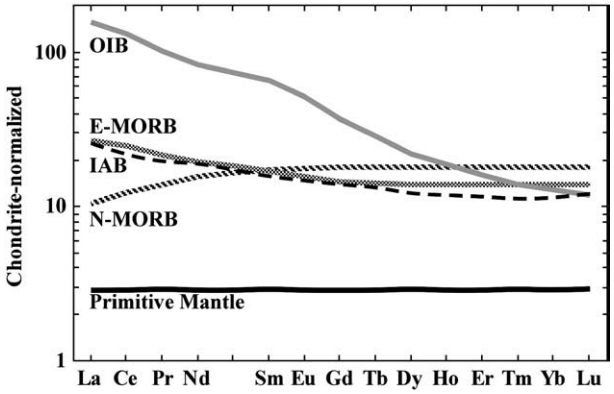

Fig. 1. Chondrite-normalized rare earth element (REE) diagram to show that average compositions of mantle derived melts as well as primitive mantle have rather smooth patterns with no Eu anomalies. Values for C1 chondrite, primitive mantle, and average compositions of ocean island basalts (OIB), N-type and E-type mid-ocean ridge basalts (MORB) are from Sun and McDonough (1989) and McDonough and Sun (1995). Average composition of island arc basalts (IAB) is from Elliott (2003). All these would imply that mantle sources for all these basalts also have smooth REE patterns without a Eu anomaly. As primitive mantle (PM) has constant values of ~2.9 times the C1 chondrite values for all REEs, subsequent REE diagrams are normalized against PM values.

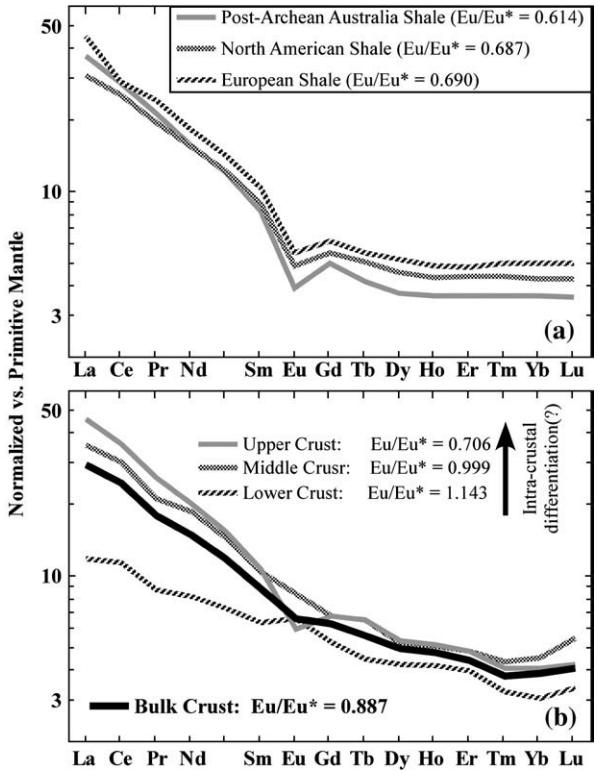

Fig. 2. (a) Upper continental crust compositions represented by shales (Taylor and McLennan, 1985) show a prominent negative Eu anomaly ($Eu/Eu^*<1$; $Eu/Eu^* = Eu_{PM}/[Sm_{PM}*Gd_{PM}]^{1/2}$, essentially identical to $2*Eu_{PM}/[Sm_{PM}+Gd_{PM}]$, where subscript $_{PM}$ denotes normalized values against PM). (b) The most up to date model compositions of upper, middle, lower and bulk continental crust by Rudnick and Gao (2003). The decreasing Eu/Eu* values from lower crust to middle and to upper crust is apparently consistent with intra-crust differentiation, but the key is that the bulk continental crust is characterized by a significant negative Eu anomaly with $Eu/Eu^* = \sim 0.887$.

2.3. Conspicuous negative Eu anomaly in the continental crust

It has long been known (Taylor and McLennan, 1985) that the upper continental crust as represented by fine-grained sediments such as loess and shales has a conspicuous negative Eu anomaly (Fig. 2a). The inference would be that the missing Eu in the upper crust may reside in the deeper crust. Fig. 2b gives model compositions of upper, middle, lower and bulk continental crust by Rudnick and Gao (2003), which is the most up-to-date painstaking effort built on works of generations (e.g., Taylor, 1967, 1977; Taylor and McLennan, 1985, 1995; Wedepohl, 1995; Rudnick and Fountain, 1995; Rudnick, 1995; Gao et al., 1998) using combined methods of petrology, geochemistry and geophysics on representative samples characterizing upper, middle and lower crust worldwide as well as sophisticated statistics. Indeed, the middle crust shows no Eu anomaly with $Eu/Eu^* = 0.999$, but the lower crust shows a large positive Eu anomaly with $Eu/Eu^* = 1.143$. The Eu/Eu* decrease from lower to middle and to upper crust is apparently consistent with intra-crustal differentiation, but the high Eu/Eu* value of the lower crust mostly results from underplated mafic magmas or their cumulate (Rudnick, 1992). Nevertheless, the bulk continental crust still has a negative Eu anomaly with $Eu/Eu^* = 0.887$, which is significant. If PM does not have a Eu anomaly (Fig. 1), where is the Eu enriched material that is complementary to the Eu deficient BCC?

2.4. Primitive MORB melts all have significant positive Eu anomalies

If we accept the first-order compositional complementarity between the BCC and DMM (e.g., Hofmann, 1988), then the missing Eu in the BCC must be in the DMM, and must also be reflected in the ocean crust that is derived from the DMM. However, it is important to note that MORB represent no more than ~15% of the oceanic crust mass (Niu, 1997), and

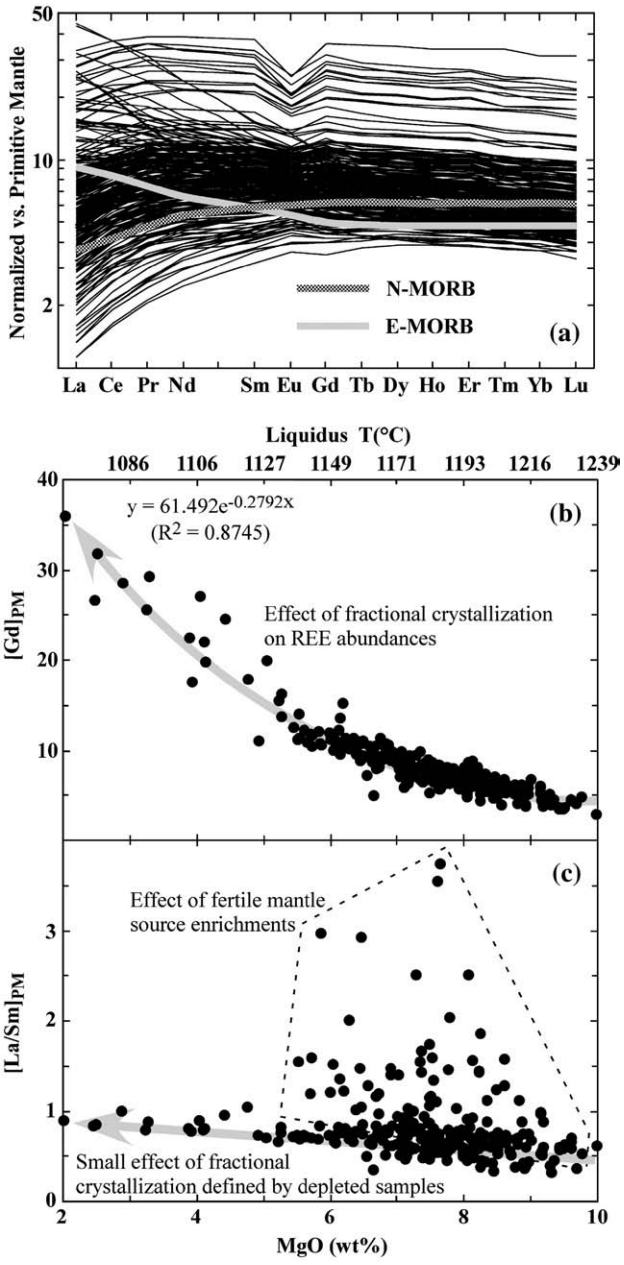

Fig. 3. (a) plots high quality MORB data on 306 fresh MORB glass samples from the East Pacific Rise ridge axis (Niu et al., 1999, 2002a; Regelous et al., 1999; Y. Niu's unpublished data) and near-axis seamounts (Niu and Batiza, 1997), the Pacific Antarctic Ridge and nearby seamounts (Castillo et al., 1998; Y. Niu's unpublished data), the Garrett Transform zone (Niu and Hékinian, 1997b; Wendt et al., 1999), the North mid-Atlantic Ridge (Niu et al., 2001) and South mid-Atlantic Ridge and nearby seamounts (Niu and Batiza, 1994; Regelous et al., 2009-this issue). Major element data of all these glasses have been analyzed using electron microprobe by Y. Niu at various institutions with inter-laboratory corrections reported in Niu and Batiza (1997). All the trace elements on these samples were analyzed using ICP-MS at The University of Queensland with analytical procedure and data precision/accuracy reported in Niu and Batiza (1997). Trace element analyses from the MORB data base (www.petdb.org) are patchy and unusable for our purpose without (1) required elements analyzed, (2) data quality control and (3) inter-laboratory comparison/correction. Our data used here in both abundances and systematics have a global spread (Niu and Batiza, 1997), thus representative of global MORB chemistry in general. (b) plots PM-normalized Gd against MgO to show that the varying REE abundances in (a) largely result from the effect of fractional crystallization with the more evolved melts (lower MgO) having higher REE abundances. (c) plots PM-normalized La/Sm to show fractional crystallization has limited effect on the La/Sm ratio, but samples with variably steep positive and negative REE patterns in (a) largely reflect mantle source compositional heterogeneity.

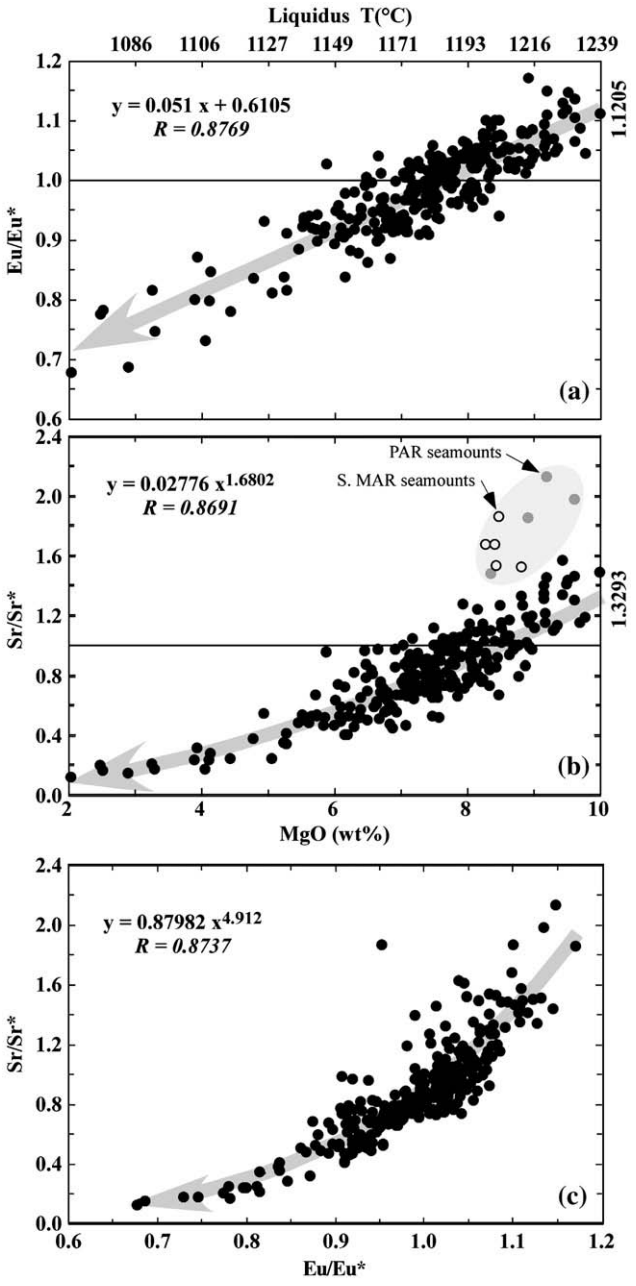

Fig. 4. (a) shows Eu/Eu* decreases linearly with decreasing MgO or liquidus temperature (indicated at the top axis, derived from Niu et al., 2002b; Niu, 2005) with ~1/2 of the samples having Eu/Eu*>1. This trend is consistent with the effect of fractional crystallization with a constant bulk D_{Eu}. Using the regression line (the thick, grey line with arrow), it is obvious that the most primitive samples in the data set with MgO = 10 wt.% have a significantly positive Eu anomaly of Eu/Eu* = ~1.1205. (b) shows that Sr/Sr* (= $2*Sr_{PM}/[Pr_{PM}+Nd_{PM}]$; see Niu et al., 1996) decreases curvilinearly (best fit in a power–law form) with decreasing MgO with ~$^1/_3$ of the samples having Sr/Sr*>1. This trend is also consistent with the effect of fractional crystallization with a bulk D_{Sr} that slightly decreases as the melt becomes more evolved with the liquidus plagioclase progressively richer in Na and poorer in Ca (Ren et al., 2003) although compositional dependence of $K_D^{Plagioclase/Melt}$ is complex (Blundy and Wood, 1991; Bédard, 2006). Decrease of modal plagioclase in the fractionating assemblage can also explain the slight D_{Sr} decrease. By excluding the few samples from the South Atlantic and Pacific Antarctic seamounts ("anomalously high" Sr/Sr*; see Regelous et al., 2009-this issue), we obtain conservatively a positive Sr anomaly of Sr/Sr* = ~1.3293 for the most primitive samples with MgO = 10 wt.%. (c) shows the correlated Eu/Eu* and Sr/Sr* variation, and emphasizes that both parameters are dictated by a common process, i.e., cooling-induced fractional crystallization of plagioclase (the effect of other minerals is insignificant in this diagram). Magma chamber processes are likely complex (O'Hara, 1977; O'Hara and Mathews, 1981; O'Hara and Herzberg, 2002), but the data show the net effect.

thus cannot be used to approximate the composition of bulk ocean crust, in particular the more compatible elements during MORB melt evolution such as Ni and Cr that are compatible in olivine, spinel and clinopyroxene and Sr and Eu^{2+} that are compatible in plagioclase. Furthermore, compositional averaging is a powerful way to reveal first-order MORB compositional systematics as a function of ridge separation rate (Niu and Hékinian, 1997a) or ridge axial depth (Klein and Langmuir, 1987; Niu and O'Hara, 2008), and to distinguish MORB from mantle melts from other tectonic settings such as OIB and IAB (Hofmann, 1988; Sun and McDonough, 1989; Niu and O'Hara, 2003). However, compositional averaging can conceal important variations that are in fact revealing (Niu and Batiza, 1997). For example, average MORB show no Eu anomaly (Fig. 1), but actual MORB melts show both positive and negative Eu anomalies (Figs. 3 and 4).

Fig. 3a shows huge variations in both abundances and patterns of actual MORB melts in contrast to the average N- and E-MORB. The varying abundance levels clearly result from MORB melt evolution as illustrated by primitive-mantle normalized Gd against MgO (Fig. 3b). That is, all REEs behave incompatibly during crystal fractionation and increase with continued cooling (decreasing MgO) and crystallization. The different patterns of some samples with light REE enrichment (i.e., $[La/Sm]_{PM}>1$) or depletion (i.e., $[La/Sm]_{PM}<1$) are largely caused by mantle source compositional variation (to a lesser extent by varying degree of mantle melting: Fig. 3c). The effect of crystal fractionation on the topology of REE patterns (i.e., $[La/Sm]_{PM}$; Fig. 3c) is rather small.

Fig. 4a shows significant linear correlation of Eu/Eu* with MgO (or liquidus temperature). Samples with Eu/Eu*>1 have MgO>7.64 wt.% or $T_{Liquidus}$>~1185 °C (~1/2 of the samples). Fig. 4b shows significant curvilinear correlation between Sr/Sr* and MgO (or liquidus temperature). Samples with Sr/Sr*>1 have MgO>8.44 wt.% or $T_{Liquidus}$>~1203 °C (~$^1/_3$ of the samples). The best fit regression gives Eu/Eu* = ~1.1205 and Sr/Sr* = ~1.3293, respectively, for the most primitive samples with MgO = ~10 wt.%. The very high Sr samples from the PAR and South MAR seamounts are excluded from the regression. These samples may be hinted at the presence of some interesting source heterogeneity (Regelous et al., 2009-this issue). Fig. 4c plots Sr/Sr* vs. Eu/Eu* showing significant curvilinear correlation between the two as expected.

2.5. The origin of Eu and Sr anomalies in MORB melts

It is already clear from Fig. 4 and foregoing discussion that the systematic Eu/Eu* and Sr/Sr* variation with MgO in MORB melts must be caused by plagioclase crystallization. We illustrate the geochemical and petrologic concepts further in Fig. 5. Fig. 5a shows experimentally determined partition coefficients of REEs and Sr for major silicate minerals involved in the generation and evolution of basaltic magmas compiled by Niu et al. (1996). Obviously, plagioclase is the only mineral that can effectively fractionate both Eu and Sr from otherwise similarly incompatible elements in other major silicate minerals (i.e., olivine, orthopyroxene, clinopyroxene; not show but also true for garnet). As Eu is much less incompatible than Sm and Gd, and Sr is much less incompatible than Pr and Nd in plagioclase, continued crystallization of plagioclase preferentially removes Eu (vs. Sm and Gd) and Sr (vs. Pr and Nd) from the residual melt, leading to the more negative Eu (Eu/Eu*<1) and Sr (Sr/Sr*<1) anomalies in the progressively more evolved (decreasing MgO) melt (Figs. 3 and 4).

Fig. 5b shows the nearly linear relationship between MgO in MORB melt and the liquidus temperature as well as liquidus mineral assemblages constructed from low-pressure (1.0 bar) experimental data (see Niu et al., 2002b; Niu, 2005). At low pressures, plagioclase begins to crystallize at MgO ~9.3 ± 0.2 wt.% (or $T_{Liquidus}$ = 1223 ± 5 °C) and continues throughout the basalt-to-basaltic andesite evolution, forming cumulate assemblages of troctolite, gabbro, oxide gabbro, gabbronorite and the more felsic lithologies. Therefore, Eu/Eu* and Sr/Sr* continue to decline with deceasing MgO in MORB melts (Figs. 3 and 4). At higher pressures, e.g., 2–3 kbars in the deep oceanic crust or upper most mantle

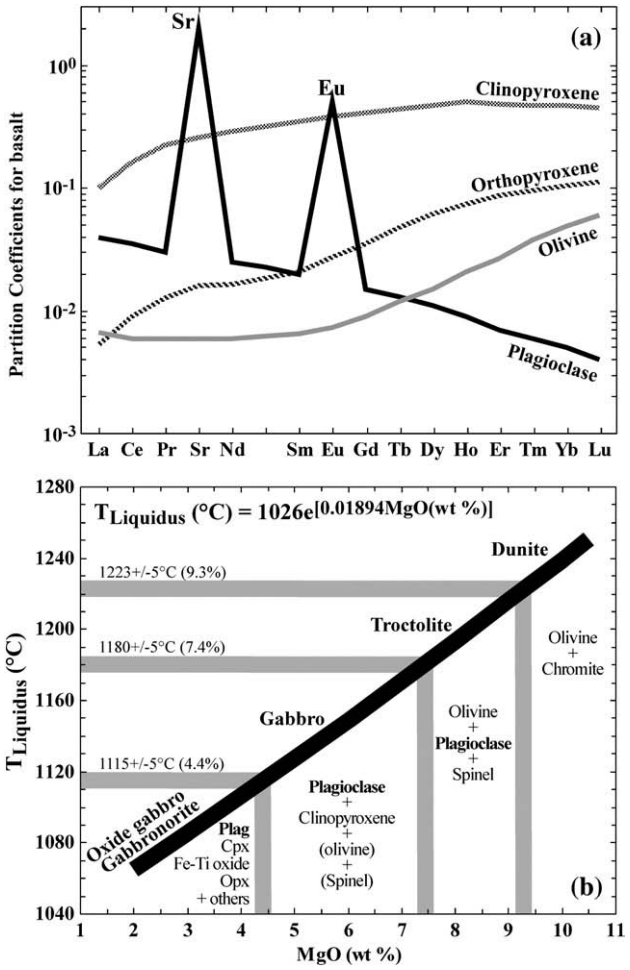

Fig. 5. (a) shows experimentally determined partition coefficients of REEs and Sr between common liquidus minerals and basaltic melts compiled by Niu et al. (1996; Table 5). Obviously, Sr and Eu are much more compatible in plagioclase (than otherwise similarly incompatible REEs) whose crystallization can effectively deplete Sr (vs. Pr and Nd) and Eu (vs. Sm and Gd) in the cooling and evolving melt. (b) plots MORB melt MgO (wt.%) and liquidus temperature at low-pressure (1 bar) constructed on experiment-based empirical models (Niu et al., 2002b; Niu, 2005). It shows that at 1 bar pressure, a primitive MORB melt crystallizes olivine (+Cr-spinel) to produce dunite until MgO = ~9.3 wt.% (or $T_{Liquidus}$ = ~1223 ± 10 °C) when plagioclase joins olivine to produce troctolite. When the melt evolves to MgO = ~7.4 wt.% (or $T_{Liquidus}$ = ~1180 ± 10 °C), clinopyroxene joins plagioclase (and olivine) to produce gabbro. When the melt MgO decreases to ~4.4 wt.% (or $T_{Liquidus}$ = ~1115 ± 10 °C), Ti–Fe oxides begin to crystallize to produce oxide gabbro, gabbronorite and norite (orthopyroxene appears on the liquidus). Clearly, continued plagioclase crystallization during MORB melt evolution explains the Sr and Eu depletion seen in Fig. 4. Note that at deep crustal level (i.e., P > 1–2 kbars), plagioclase would begin to crystallize at a higher temperature (e.g., Langmuir et al., 1992).

conditions, liquidus phases may appear earlier at higher liquidus temperatures (higher MgO also) (e.g., Langmuir et al., 1992). The key observation is that all samples with MgO > 9.5 wt.% have excess Eu (Eu/Eu* > 1) and Sr (Sr/Sr* > 1), pointing to the fact that "primary" MORB melts must have excess Eu and Sr. As expected, the oceanic lower crustal gabbros (Niu et al., 2002b) and model bulk ocean crust do have strong positive Eu anomalies (see Fig. 19a of Niu, 2004). That is, under normal conditions, Moho-crossing mantle melts must have significant positive Eu and Sr anomalies. Preferential diffusion of Sr as a result of melt-gabbro assimilation in the lower crust may lead to Sr enrichment in the melt (e.g., Saal et al., 2007), but this cannot explain the correlated Sr/Sr*–Eu/Eu*–MgO variations defined by the global MORB data (Fig. 4).

2.6. The DMM has excess Eu and Sr

One may argue that primitive, Moho-crossing MORB melts may gain their excess Eu and Sr by absorbing Ca-rich plagioclase in the mantle. As excess Eu and Sr exists in all sample suites from both ridge axis and near-ridge seamounts in both Pacific and Atlantic ocean basins, the suspect plagioclase absorption would have to be a universal process. The question then is where and how the invoked plagioclase forms and resides. One could argue that the candidate plagioclase naturally occurs in the plagioclase peridotite facies beneath ocean ridges. However, the equivalent sub-ridge mantle regime is occupied by advanced MORB melting residues without plagioclase, but spinel harzburgite as manifested by abyssal peridotites (Dick, 1989; Niu and Hékinian, 1997b). Plagioclase, if any at all, is precipitated from rather cooled melts at very shallow depths (Hékinian et al., 1995; Niu and Hékinian, 1997b). In this context, it is important to note that the "plagioclase-peridotite facies" depth range is equivalent to the cold thermal boundary layer beneath ocean ridges, where no melting occurs (Niu, 1997, 2004). Elsewhere, this depth range is within the lithosphere. Therefore, mantle peridotite melting in the "plagioclase peridotite stability field" is an interesting concept, but is physically unlikely (Niu, 2004). It follows that the excess Eu and Sr in primitive or "primary" MORB melts are inherited from the DMM source. Because the primitive mantle has no Eu (and Sr) anomaly (Fig. 1), then the excess Eu and Sr in the DMM accounts for the deficiency of these two elements in the continental crust. It should be noted that Sobolev et al. (2000) interpreted the composition of olivine melt inclusions in some Hawaiian lavas as recording "ghost" plagioclase of ancient recycled gabbros, which apparently favors our argument for the presence of excess Sr and Eu in the mantle source. However, as their host olivine is a liquidus phase crystallized from the cooling and evolving melts in crustal magma chambers, the trapped melt cannot be primary melt in equilibrium with mantle minerals (Niu and O'Hara, 2003). Hence, caution is necessary when using olivine melt inclusions to infer mantle sources/processes.

3. Discussion

The recognition of excess Eu and Sr in primitive MORB melts and their likely residence in the DMM corroborates the view that the DMM complements the bulk continental crust (BCC). This recognition also offers new perspectives on two of the fundamentally important solid Earth problems that we explore here, namely, the origin of the continental crust and the chemical structure of the oceanic upper mantle.

3.1. On the origin of continental crust and crust–mantle differentiation

While the BCC composition is reasonably well established (Rudnick and Gao, 2003), a genuine understanding of its origin, mode and rate of accretion, and how it has acquired its "andesite" bulk composition from mantle derived materials remains speculative (e.g, Rudnick and Gao, 2003; Kelemen et al., 2003a,b; Plank, 2005; Davidson and Arculus, 2006). The first-order compositional complementarity between the BCC and DMM in general and that of Eu and Sr in particular offers new insights into processes of continental crust accretion. A straightforward implication is that the process of continental crustal formation from mantle derived melts involves plagioclase because the latter is the only mineral phase that is known to be able to effectively, simultaneously and consistently fractionate Eu and Sr from other elements (e.g., Sun et al., 1974). The melting process is such that plagioclase is a residual phase that preferentially holds Sr and Eu. The melt that is thus depleted in these two elements accretes to the continental crust, resulting in the weak but significant negative Sr and Eu anomalies in the BCC. Given the fact that calcic plagioclase (vs. Na-rich compositions) is rather refractory, the residual plagioclase is likely to become more Ca-rich, and would hold more Eu and Sr. This is because Eu^{2+} and Sr^{2+} prefer to substitute for Ca^{2+} (vs. Na^{+}) (i.e., similar charge-to-radius ratios: $R^{Eu^{2+}}_{CN=6} = 1.709 \approx R^{Sr^{2+}}_{CN=6} = 1.695 \approx R^{Ca^{2+}}_{CN=6} = 2.000$ vs. $R^{Na^{1+}}_{CN=6} = 0.980$; Shannon, 1976). Indeed, a positive correlation exists between Sr and anorthite contents in plagioclase (e.g., Blundy and

Wood, 1991; Izbekov et al., 2002; Pietranik et al., 2006). This requires that the Ca-rich plagioclase residue stay in or return to the convective mantle and its chemical imprint be identified in the DMM. This reasoning is consistent with the hypothesis "continental collision zones, *not active subduction zones*, are primary sites of net continental crustal growth" (Niu et al., 2007; Mo et al., 2008), whose concept will become clear later in the section. This hypothesis does not tell us when and how the proto-type continental crust may have formed, but can effectively explain the composition of the BCC as well as its growth in the context of plate tectonics. Given the fact that the origin of continental crust is one of the oldest remaining major problems we continue to face, it is necessary to briefly review the prevailing theory and its shorting-comings, which led to our new hypothesis.

3.1.1. The prevailing model and its shortcomings

Most models suggest that the continental crust has been growing continuously over Earth's history by means of adding mantle derived magmas (see Condie, 2005). Compared to rocks formed from mantle derived magmas in all geological environments, island arc rocks associated with oceanic lithosphere subduction share some common features with the BCC; both are depleted in "fluid-insoluble" elements (e.g., Nb, Ta and Ti), but enriched in "fluid-soluble" elements (e.g., U, K and Pb). These chemical characteristics are referred to as the "arc-like signature", and point to a genetic link (Taylor and McLennan, 1985) between subduction-zone magmatism and continental crust formation, thus leading to the "island arc" model (Taylor, 1967, 1977) widely accepted for the origin of continental crust. For example, it is believed that juvenile continental crustal materials may indeed be forming at present along island arcs such as the Izu–Bonin–Mariana arc system in the western Pacific (e.g., Takahashi et al., 2007). However, this "Island-arc" model has many more difficulties than certainties.

The bulk arc rocks are basaltic and are thus too mafic (e.g., Gill, 1981; Arculus, 1981; Pearcy et al., 1990) for the andesitic BCC. Removal of mafic/ultramafic lower arc crust cumulate beneath active arc or during orogenesis is a popular idea (e.g., Kay and Kay, 1993; Rudnick, 1995; Kelemen et al., 2003a; Plank, 2005) to explain why only felsic arc lithologies contribute to continental crust, although the perceived physical mechanisms for such removal may be complex (Jull and Kelemen, 2001). An alternative interpretation requires no physical separation of the mafic/ultramafic cumulate from the overlying andesitic lithologies, but argues that the apparent conflict lies in our perception of the felsic crust above the Moho and the mafic/ultramafic cumulate beneath the Moho in the mantle because the Moho is a seismic, not petrologic, division (Davidson and Arculus, 2006). However, xenolith studies show no evidence for such cumulate beneath the Moho unless they may have been removed subsequently by density foundering (e.g., Rudnick and Gao, 2003) or other unknown dislocation processes (Davidson and Arculus, 2006).

Slab melting and melt–mantle interactions are thought to be an important mechanism to produce high magnesian andesites (HMA vs. basaltic melts) resembling the BCC composition (Kelemen, 1995; Kelemen et al., 2003b; Tatsumi, 2006). However, this requires not only warm slabs but also unusually hot mantle wedge that is rare at present (Tatsumi, 2006). Likewise, adakites (Defant and Drummond, 1990) are a variation of HMA with the "garnet-signature" resembling the more abundant TTG suite produced in the Archean when the mantle was hotter. Present-day adakites, once thought to be unique product of slab melting, can in fact be formed in different tectonic settings by various means (Castillo, 2006). In any case, bulk arc crust is basaltic, *not* andesitic. Note also that while Archean TTGs may be important in helping understand the origin of the "proto-type" continental crust, the fact that the BCC composition (Rudnick and Gao, 2003) shares no chemical property of the TTGs suggests that the TTGs are volumetrically unimportant in building the present-day continental crust mass.

Importantly, island arc basalts (also bulk arc crust) have variably large excess Sr (Sr/Sr* is up to ~6) derived from altered ocean crust (Staudigel, 2003) during subduction that decouples from the limited Eu/Eu* variation (0.8 to 1.3) (Fig. 6). Plagioclase fractionation (the dashed lines) can readily reduce Eu excesses (in the case of Eu/Eu*>1) to the mean value of 0.887, but cannot in anyway reduce Sr/Sr* to match the mean value of 0.933 for the BCC (Fig. 6). The Sr argument alone suggests that island arc rocks are wrong material for the BCC composition.

In addition, it has been showed that island arc crust production is mass balanced by subduction erosion and sediment recycling (von Huene and Scholl, 1991; Scholl and von Huene, 2004; Clift and Vannucchi, 2004) on modern Earth. Furthermore, isotopic studies demand that crustal recycling at subduction zones has been important since ~2.0 Ga (Armstrong, 1968; Kramers and Tolstikhin, 1997). Therefore, active subduction zones may not be sites for net continental growth, thus contributing no new mass to the continental crust, at least in the past >200 million years (Clift and Vannucchi, 2004). Nevertheless, continental crust-like materials may indeed be forming at present at some arcs such as the Izu–Bonin–Mariana arc system (e.g., Tatsumi, 2006; Takahashi et al., 2007), although it is not straightforward how intra-oceanic arcs contribute to continental growth without continental collision or terrain accretion because they are moving away from continents; back arc basins spread and ocean basins spread also.

3.1.2. Continental collision zones as primary sites for net continental crust growth

This new concept is developed on the basis of recent (Niu et al., 2007; Mo et al., 2008) and ongoing studies of rocks in southern Tibet formed during the India–Asia continental collision some 60 million years ago. This hypothesis considers all the observations and logical interpretations that are summarized here.

During or soon after initial continental collision (ocean basin closing), the last bit of ocean crust will continue to underthrust at a retarded rate. This slow underthrust facilitates its thermal equilibrium to reach amphibolite conditions.

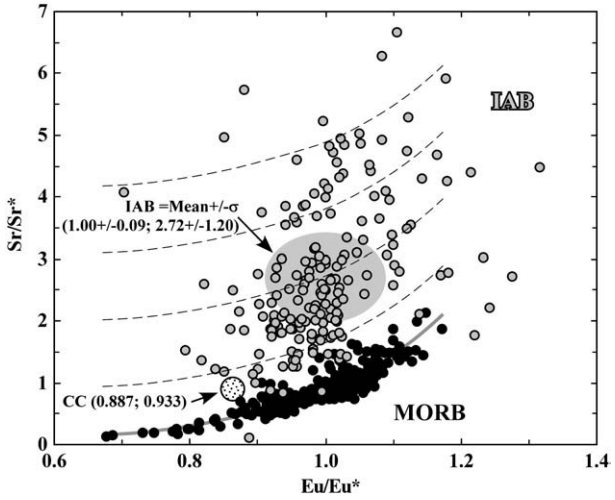

Fig. 6. Comparison of MORB (this study, see Fig. 4c) with island arc basalts (IAB) (Elliott, 2003) in Sr/Sr* vs. Eu/Eu* space. The variably large positive Sr anomalies are characteristic of IAB, and are significantly greater than those of MORB. The variably high Sr contents in IAB are consistent with IAB resulting from subducting slab dehydration-induced mantle wedge melting and Sr being an important slab component (Elliott, 2003) originated from altered oceanic crust (Staudigel, 2003). The dashed lines drawn parallel to the data trend defined by MORB is the fractionation trend due to plagioclase only (effect of all other liquidus minerals is insignificant). Hence, plagioclase fractionation cannot reduce the high Sr/Sr* values in IAB. Therefore, neither IAB nor their evolved derivatives can be candidate for continental crustal material in terms of Sr; continental crust has a weak negative, NOT large positive, Sr anomaly (See Table 1 and Fig. 8).

The amphibolite of MORB protolith begins to melt when reaching the wet basaltic solidus (Stern et al., 1975; Wyllie and Wolfe, 1993; Wolf and Wyllie, 1994; Rapp, 1995; Rapp and Watson, 1995); the ocean crust is hydrated by hydrothermal alteration at ocean ridges and by subsequent seafloor weathering.

Partial melting of the amphibolite produces melt of andesitic composition (both volcanic and giant batholiths), resembling the BCC. This melt inherits its mantle isotopic signature (i.e., elevated $\varepsilon_{Nd(t)}$ of −2 to +9.0 with most samples having $\varepsilon_{Nd(t)}>0$ in contrast to $\varepsilon_{Nd(t)}<-12$ of mature continental crust) from the ocean crust produced recently at an ocean ridge, thus representing juvenile mantle-derived material contributing to the continental crust mass. This juvenile crust is well preserved in the collision zones.

Typical amphibolite of MORB protolith consists of amphibole, plagioclase, ilmenite (or pseudobrookite) and a few other minor phases (Niu and Lesher, 1991). Ilmenite as a residual phase, together with residual amphibole, accounts for the depletion of Nb, Ta and Ti in the melt. Residual amphibole that also possesses super-chondritic Nb/Ta ratio explains the more sub-chondritic Nb/Ta ratio in the melt. Residual plagioclase explains the slightly depleted, *not* enriched, Sr (and Eu) in the melt, typical of continental crust. The effect of ocean crust alteration plus involvement of mature crustal materials (e.g., recycled terrigeneous sediments) enhances the abundances of Ba, Rb, Th, U, K and Pb in the melt.

As the syncollisional process of juvenile crust formation derives magmas from the ocean crust atop the subducting/underthrusting oceanic lithosphere within the mantle, the more mafic residue of ocean crust melting remains in the mantle, which circumvents the need of the otherwise unknown processes to convert the more mafic arc assemblage to the andesitic continental crust required by the "island arc" model. The residual ocean crust after melt extraction continues to enter the deep mantle along with the subjacent oceanic lithosphere.

Partial melting of the ocean crust at amphibolite conditions (<40 km) explains the lack of "garnet signature" in the composition of the BCC, and also the so-called "arc-like signature" (not for Sr; see Fig. 6 and above discussion).

These observations and reasoning plus the remarkable compositional similarity between the syncollisional andesite and the BCC (see Fig. 8 of Mo et al., 2008) make the syncollisional magmatism a genuine continental crust mass contributor. Robust and fully quantitative geochemical modelling of the melting process cannot yet be done because existing melting experiments on amphibolite or similar rocks

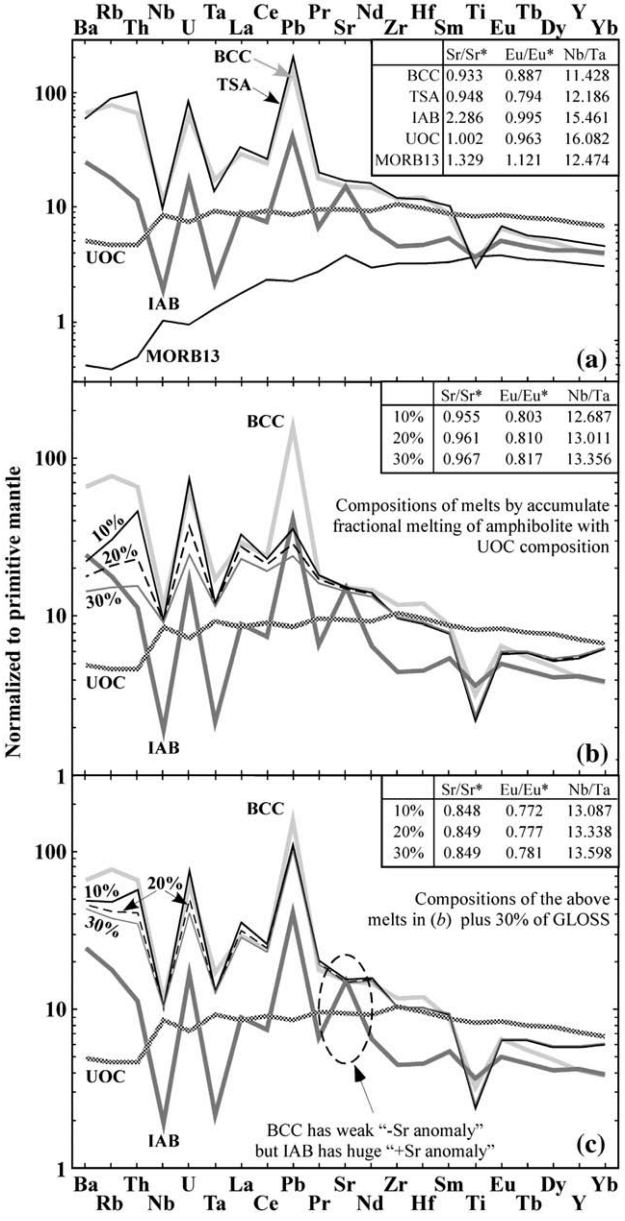

Fig. 7. (a) Primitive mantle (PM) normalized multi-element diagram to compare compositions of bulk continental crust (BCC; Rudnick and Gao, 2003), Tibetan syncollisional andesite (TSA; Mo et al., 2008), upper oceanic crust (UOC) made of 75% N-type MORB and 25% E-type MORB (Niu and O'Hara, 2003), average island arc basalts (IAB; Elliott, 2003) and MORB13, which is our robust model composition of depleted primitive or "primary" MORB melt with 13 wt.% MgO, and is obtained by the following: (1) We obtained apparent liquid lines of descent (LLDs) for all these elements on MgO variation diagrams (e.g., for $[Gd]_{PM}$ in Fig. 3b, but un-normalized) by plotting all the samples with $[La/Sm]_{PM}\leq 1$; (2) the LLDs of all these elements fit an exponential equation of the form $Y=ae^{(bX)}$ with $R>0.90$; (3) this equation is used to obtain the concentration of each element (Y in ppm) at X = MgO = 10 wt.% (the most primitive sample available; see Figs. 3 and 4). The best fit coefficients are: $a_{Ba}=220.9$, $b_{Ba}=-0.4252$; $a_{Rb}=31.22$, $b_{Rb}=-0.4773$; $a_{Th}=4.894$, $b_{Th}=-0.4689$; $a_{Nb}=70.19$, $b_{Nb}=-0.4502$; $a_{U}=1.801$, $b_{U}=-0.4442$; $a_{Ta}=4.272$, $b_{Ta}=-0.4304$; $a_{La}=57.36$, $b_{La}=-0.3783$; $a_{Ce}=157.9$, $b_{Ce}=-0.3588$; $a_{Pb}=5.144$, $b_{Pb}=-0.3392$; $a_{Pr}=25.22$, $b_{Pr}=-0.3450$; $a_{Nd}=111.0$, $b_{Nd}=-0.3241$; $a_{Zr}=1202$, $b_{Zr}=-0.3431$; $a_{Hf}=30.99$, $b_{Hf}=-0.3363$; $a_{Sm}=30.81$, $b_{Sm}=-0.2965$; $a_{Ti}=60637$, $b_{Ti}=-0.2462$; $a_{Tb}=6.018$, $b_{Tb}=-0.2708$; $a_{Dy}=39.72$, $b_{Dy}=-0.2686$; $a_{Y}=210.4$, $b_{Y}=-0.2596$; $a_{Yb}=22.55$, $b_{Yb}=-0.2636$. Eu and Sr are constrained by $Eu/Eu^*=1.1025$ and $Sr/Sr^*=1.3293$ at MgO = 10 wt.% (Fig. 4); (4) assuming that a "primary" MORB melt in equilibrium with mantle peridotite has ~13 wt.% MgO (Niu, 1997; Niu and O'Hara, 2003), that the mantle melt crystallizes olivine (plus Cr-spinel) only from 13% to 10% MgO (Fig. 5) without consuming significant amounts of these incompatible elements, and that the olivine has an average composition of ~50 wt.% MgO (i.e., Fo ~ 0.908), we thus obtained $f_{Ol}=(13-10)/(50-10)=0.075=7.5\%$ olivine crystallization from the original melt mass. Dilution of the MORB melt with 10% MgO by adding 7.5% olivine, we obtain the MORB13. (b) Shows model calculations of aggregated melt compositions of 10%, 20% and 30% fractional melting (similar to batch melting compositions) of our model UOC (Niu and O'Hara, 2003) (see Table 1) under amphibolite facies conditions (see Mo et al., 2008). Simplified mineral modes of the amphibolite of MORB protolith (Table 1) are taken from Niu and Lesher (1991): 66.4 wt.% "hornblende" (including minor chlorite, biotite and epidote), 4.4 wt.% ilmenite/pseudobrookite and 29.2 wt.% "plagioclase" (also including minor quartz and calcite). Partition coefficients between these major phases and basaltic andesite/andesite melts for all elements are also detailed in Table 1. Note that although partial melting of multi-component natural systems is incongruent "non-modal" melting, without knowing melting reaction and melting modes we use simple modal melting to illustrate the concept. Although calculated model melts do not match well the abundance levels of the BCC, they do capture the characteristic features of continental crust, e.g., relative enrichments in Ba, Rb, Th, U and Pb, relative depletion of Nb, Ta and Ti as well as weak negative Sr and Eu anomalies, and the more sub-chondritic Nb/Ta ratio (even lower than 16.1 of the source rocks UOC). (c) Isotopically (in terms of $\varepsilon_{Nd(t)}$, see Mo et al., 2008), the syncollisional Tibetan andesite (TSA) indicates 10 to 30% terrigeneous sediments involvement, likely in the melting region during the subducting/underthrusting of the Tethyan ocean crust upon India–Asia collision. While sediment melting experiments have been carried out to illustrate the phase stability (Nichols et al., 1994; Johnson and Plank, 1999), no ideal melting reactions with detailed melting modes available to quantify sediment melting. However, for conceptual illustration on the effect of sediment involvement, we can simply add ~30% of the global subducting sediment (GLOSS) (Plank and Langmuir, 1998) to the model melts in (b). The results of MORB melting (in the amphibolite facies) with sediment involvement produce new melt compositions that match the BCC composition well. Note that addition of GLOSS is required by the TSA to explain the isotopic data, and in practice such sediments on deep trench seafloor is readily available for underthrusting along with the ocean crust and syncollisional melting. Note also that the huge positive Sr anomaly makes Island arc rocks (e.g., IAB) unsuitable for continental crust.

are limited to phase stability, which does not yet allow parameterization of melting reactions and melting mode proportions necessary for both major and trace elements modelling. Nevertheless, Mo et al. (2008) carried out some simple melting calculations to illustrate that partial melting of amphibolite of MORB protolith can reproduce important geochemical properties of continental crust. They focused on Th, Nb, U, Ta and La). In the next section, we consider a spectrum of elements and show that the weak, but significant Eu and Sr deficiency, as well as Nb, Ta and Ti deficiencies, in the BCC can be produced by melting of amphibolite of MORB protolith.

3.1.3. Melt composition of wet MORB melting under amphibolite facies conditions

Fig. 7a compares the composition of the BCC, average Tibetan syncollisional andesite (TSA), average island arc basalt (IAB), upper oceanic crust (UOC) and our robust model composition of depleted primitive MORB melt with 13% MgO (MORB13; see Fig. 7a caption for details) on primitive mantle normalized multi-element diagram. The remarkable compositional (both major and trace elements) similarity of the TSA and BCC led to the hypothesis (Niu et al., 2007; Mo et al., 2008) that continental collision zones are primary sites of net continental crust accretion. The mantle isotopic signature of the TSA (i.e., elevated $\varepsilon_{Nd(t)}$ values with most samples having $\varepsilon_{Nd(t)}>0$) allow these authors to suggest further that the TSA result from partial melting of the last bit of the Tethyan ocean crust during the India–Asia collision because it is the ocean crust recently formed at an ocean ridge that carries the mantle isotopic signature. These authors also emphasize that the bulk ocean crust (Niu and O'Hara, 2003) is too depleted (because of the more depleted cumulate lower crust) as the source to produce the incompatible element enriched TSA (Fig. 7a). However, partial melting of the UOC of "melt composition" (i.e., lavas and feeder dikes) under amphibolite facies conditions is required. Our preferred UOC is the combination of 75% average N-MORB and 25% average E-MORB (Niu and O'Hara, 2003) hydrothermally altered at ocean ridges and subsequently weathered on the seafloor. Although partial melting of multi-component natural systems is incongruent "non-modal" melting, without knowing melting reaction with melting modes, we use simple modal melting models to illustrate the concept.

Table 1
Average and model compositions (normalized to primitive mantle) and relevant partition coefficients.

	PM [1]	BCC [2]	TSA [3]	IAB [4]	UOC [5]	MORB13 [6]	GLOSS [7]	Model melt (10%FM) [8]	Model melt (20%FM) [9]	Model melt (30%FM) [10]	10% FM+0.3 GLOSS [11]	20% FM+0.3 GLOSS [12]	30% FM+0.3 GLOSS [13]	Amphibole 0.664	[14]	Plagioclase 0.292	[14]	Ilmenite/ Pseudo-brookite 0.044	[14]	Bulk D [15]
Ba	6.989	65.25	60.29	24.66	4.993	0.416	111.0	22.22	17.79	14.37	48.86	45.76	43.37	0.120	[16]	0.340	[21]	0.000	[24]	0.179
Rb	0.635	77.17	92.00	17.96	4.656	0.385	90.08	30.39	20.80	15.09	48.29	41.58	37.58	0.140	[16]	0.023	[22]	0.000	[24]	0.100
Th	0.085	65.88	105.0	11.40	4.626	0.490	81.29	46.24	23.13	15.42	56.75	40.58	35.18	0.017	[16]	0.010	[23]	0.001	[25]	0.014
Nb	0.713	11.22	9.78	1.922	8.594	1.010	12.54	13.26	12.84	12.40	13.04	12.75	12.44	0.853	[17]	0.022	[22]	1.272	[25]	0.629
U	0.021	61.90	87.75	16.66	7.369	0.934	80.00	73.69	36.85	24.56	75.58	49.79	41.19	0.008	[16]	0.010	[23]	0.006	[25]	0.008
Ta	0.041	17.07	13.95	2.162	9.293	1.302	15.37	18.18	17.16	16.15	17.33	16.62	15.91	0.609	[17]	0.027	[22]	1.629	[25]	0.484
La	0.687	29.11	34.23	8.899	8.557	1.757	41.92	33.12	27.61	23.08	35.76	31.91	28.74	0.245	[18]	0.180	[22]	0.000	[26]	0.215
Ce	1.775	24.23	26.97	7.441	9.210	2.275	32.28	23.19	21.14	19.20	25.92	24.48	23.12	0.485	[18]	0.140	[22]	0.007	[26]	0.363
Pb	0.071	154.9	211.1	41.03	8.521	2.254	280.3	35.37	28.92	23.78	108.8	104.3	100.7	0.120	[16]	0.400	[22]	0.000	[24]	0.196
Pr	0.276	17.75	20.77	6.700	9.588	2.683	26.11	18.12	17.17	16.23	20.51	19.86	19.19	0.700	[18]	0.130	[22]	0.008	[26]	0.503
Sr	21.10	15.17	17.65	15.12	9.479	3.756	15.50	15.38	14.82	14.25	15.42	15.03	14.62	0.280	[16]	1.400	[22]	0.004	[25]	0.595
Nd	1.354	14.77	16.49	6.530	9.333	2.968	19.94	14.11	13.68	13.25	15.86	15.56	15.25	0.915	[18]	0.120	[22]	0.008	[26]	0.643
Zr	11.20	11.79	12.36	4.515	10.56	3.212	11.61	9.734	9.779	9.827	10.30	10.33	10.36	1.564	[19]	0.014	[19]	1.054	[25]	1.089
Hf	0.309	11.97	11.95	4.607	9.723	3.212	13.14	9.010	9.048	9.091	10.25	10.28	10.31	1.534	[19]	0.014	[19]	1.390	[25]	1.084
Sm	0.444	8.784	10.38	5.415	8.845	3.311	13.02	7.764	7.819	7.881	9.340	9.379	9.422	1.690	[18]	0.083	[22]	0.009	[26]	1.147
Ti	1300	3.228	2.972	3.691	8.194	3.680	2.859	2.190	2.284	2.393	2.391	2.457	2.533	5.175	[18]	0.047	[22]	10.00	[24]	3.890
Eu	0.168	6.548	6.992	5.057	8.378	3.772	7.798	5.820	5.925	6.041	6.414	6.487	6.568	1.620	[18]	1.326	[19]	0.008	[26]	1.463
Gd	0.596	6.208	7.477	4.768	8.549	3.423	8.826	6.764	6.847	6.939	7.382	7.441	7.505	1.895	[18]	0.067	[22]	0.008	[26]	1.278
Tb	0.108	5.556	5.778	4.595	8.019	3.436	7.798	5.869	5.962	6.064	6.448	6.513	6.584	2.060	[18]	0.061	[22]	0.009	[26]	1.386
Dy	0.737	4.885	5.462	4.172	7.748	3.397	6.771	5.300	5.398	5.508	5.741	5.810	5.887	2.225	[18]	0.031	[22]	0.010	[26]	1.487
Ho	0.164	4.695	5.049	4.059	7.459	3.297	6.427	5.407	5.494	5.591	5.713	5.774	5.842	2.098	[18]	0.024	[22]	0.012	[26]	1.400
Y	4.550	4.176	5.046	4.214	7.223	3.188	6.549	5.479	5.557	5.643	5.800	5.855	5.915	2.000	[20]	0.024	[22]	0.012	[26]	1.335
Er	0.480	4.375	4.621	3.972	7.341	3.239	6.083	5.658	5.735	5.819	5.786	5.839	5.898	1.970	[18]	0.016	[22]	0.016	[26]	1.313
Tm	0.074	3.784	4.378	3.808	6.814	3.100	5.841	5.735	5.789	5.847	5.767	5.804	5.845	1.798	[18]	0.014	[22]	0.020	[26]	1.198
Yb	0.493	3.854	4.630	3.925	6.773	3.032	5.598	6.277	6.304	6.334	6.074	6.093	6.113	1.625	[18]	0.011	[22]	0.025	[26]	1.083
Lu	0.074	4.054	4.586	4.099	6.730	3.028	5.581	7.256	7.222	7.187	6.753	6.730	6.705	1.385	[18]	0.009	[22]	0.029	[26]	0.924
Eu/Eu*		0.887	0.794	0.995	0.963	1.121	0.727	0.803	0.810	0.817	0.772	0.777	0.781	0.905		17.78		1.003		1.209
Sr/Sr*		0.933	0.948	2.286	1.002	1.329	0.673	0.955	0.961	0.967	0.848	0.849	0.849	0.347		11.20		0.513		1.038
$[Ti/Sm]_{PM}$	1.000	0.368	0.286	0.682	0.926	1.111	0.220	0.282	0.292	0.304	0.256	0.262	0.269	3.062		0.563		1099		3.392
$[Nb/Th]_{PM}$	1.000	0.170	0.093	0.169	1.857	2.061	0.154	0.287	0.555	0.804	0.230	0.314	0.354	50.16		2.200		1817		44.15
$[Ta/U]_{PM}$	1.000	0.276	0.159	0.130	1.261	1.395	0.192	0.247	0.466	0.657	0.229	0.334	0.386	76.15		2.700		285.8		57.07
Nb/Ta	17.39	11.43	12.19	15.46	16.08	12.47	14.19	12.69	13.01	13.36	13.09	13.34	13.60	1.400		0.815		0.781		1.299

[1] Primitive mantle composition (Sun and McDonough, 1989; McDonough and Sun, 1995); [2] Model composition of bulk continental crust (Rudnick and Gao, 2003); [3] Average of Tibetan syncollisional andesite (Mo et al., 2008); [4] Average island arc basalts (Elliott, 2003); [5] Model upper oceanic crust composition calculated by combining 75% N-type MORB and 25% E-type MORB (Niu and O'Hara, 2003), representing mean compositions of global MORB lavas (Seismic Layer 2a) and feeding/sheeted dikes (Seismic Layer 2b); [6] A robust model composition of depleted primitive or "Primary" MORB melt with MgO = 13 wt.% (see text); [7] model composition of global subducting sediment (GLOSS; Plank and Langmuir, 1998); [8–10] Model compositions of aggreagate melts by 10%, 20% and 30% modal accumulate fractional melting of OUC ([5]) under amphibolite facies conditions (Niu and Lesher, 1991) using the modes in [14], partition coefficients ([16–26]) and bulk distribution coefficients ([15]); [11–13]. Compositions of model melts ([8–10]) plus 30% of GLOSS ([7]) to illustrate conceptually the effects of sediment contributions to melt compositiosn of OUC melting. By adding the GLOSS in the melting region would be more realistic, but there is no sediment melting reaction available as yet for this more rigorious treatment; [14] mineral modes of amphibolite of MORB protolith (Niu and Lesher, 1991), where for conceptual colarity 66.4 wt.% "hornblende" also includes minor chlorite, biotite and epidote, 4.4 wt.% ilmenite may in fact be ilmenite-pseudobrookite solid solutions, and 29.2 wt.% plagioclase also includes minor quartz and calcite); [15] Bulk D = mode-weighted sum of individual Kd values. Note that the greater "bulk D" for "Eu/Eu*" > 1 and "Sr/Sr*" > 1 ensure observable negative Sr and Eu anomalies in the melt, for "Nb/Th" >>1 and "Ta/U" >>1 leads to Nb and Ta depletion in the melt, and "Nb/Ta" > 1 results in the more subchondritic Nb/Ta ratios (<< 17.39) in the resultant melt required for continental crust; [16] data from Brenan et al. (1995); [17] Derived from an excellent data set confidently projected to bulk rock SiO_2 = 60% (Tiepolo et al., 2000); [18] Data from Klein et al. (1997); [19] Data from Fujimaki et al. (1984); [20] Inferred from Kd's of Ho and Er; [21] Data from Drake and Weill (1975); [22] Data from Dunn and Sen (1994); [23] Dostal et al. (1983); [24] Assumed; [25] Data from Klemme et al. (2006); [26] Data and interpolations from Nielsen et al. (1992).

We use the amphibolite modal mineralogy of Niu and Lesher (1991), i.e., ~66.4% amphibole, ~4.4% ilmenite (and pseudobrookite) and ~29.2% plagioclase and experimentally determined partition coefficients between these phases and andesite (or basaltic andesite) detailed in Table 1.

Fig. 7b shows melt compositions of 10%, 20% and 30% accumulated fractional melting (similar to batch melting results) from amphibolite of UOC composition along with the BCC and IAB on primitive mantle normalized multi-element diagram. While the abundances of the progressively more incompatible elements of the model melts do not well match those of the BCC, they do capture the key features such as the relative depletion of Nb, Ta and Ti and relative enrichment of Th, U, La and Pb as well as the more sub-chondritic Nb/Ta ratio of <13 (vs. 16.1 of the UOC and chondritic value of 17.4) characteristic of continental crust. Isotopically, the TSA, though dominated by mantle signatures (i.e., elevated $\varepsilon_{Nd(t)}$ values; see above), indicates 10 to 30% terrigeneous sediments involvement (Mo et al., 2007, 2008), likely in the melting region during the subducting/underthrusting of the Tethyan ocean crust upon India–Asia collision. While sediment melting experiments have been carried out to illustrate the phase stability (Nichols et al., 1994; Johnson and Plank, 1999), no ideal melting reactions with detailed melting stoichiometry available to quantify sediment melting. However, for conceptual illustration on the effect of sediment involvement, we can simply add ~30% of the global subducting sediment (GLOSS) (Plank and Langmuir, 1998) to the model amphibolite melts (Fig. 7b). Fig. 7c shows the results, which capture both the abundances and patterns of the BCC quite well. The calculation details are also given in Table 1.

The above exercise, although not yet ideal without adequate experimental data on incongruent melting reactions of amphibolite and sediments, can illustrate the concept that amphibolite melting of MORB protolith with sediment addition can produce the BCC composition well. In other words, this syncollisional ocean crust melting under amphibolite facies conditions can produce the required "arc-like signature" of the continental crust without invoking active subduction of oceanic lithosphere and related island arc magmatism. To be more precise, continental crust does not have the exact "arc-like signature", which includes variably large Sr excess (Figs. 6 and 7). If anything, the BCC has a weak Sr deficiency (i.e., Sr/Sr* ~ 0.993<1) as do model melt compositions with and without sediments addition (Fig. 7, Table 1).

3.1.3.1. The origin of negative Nb, Ta and Ti anomalies and the more sub-chondritic Nb/Ta ratio in the continental crust. The foregoing simple calculations illustrate that the negative Nb, Ta and Ti anomalies in the model melts (Fig. 7, Table 1) result from greater bulk distribution coefficients of these elements relative to otherwise similarly incompatible elements if the melting were taking place in the mantle beneath ocean ridges or oceanic islands (Niu and Batiza, 1997; also see below). Specifically, $D^{Nb/Th}>40$, $D^{Ta/U}>50$ and $D^{Ti/Sm}>3$ (see Table 1), which are largely controlled by amphibole (to a lesser extent by ilmenite) because of its high Kd's and high modal proportion (~66.4%). It is also amphibole with $Kd^{Nb/Ta}_{Amp}=1.40$ (Foley et al., 2002) (thus $D^{Nb/Ta}=1.30$) that explains the even lower Nb/Ta (~13) in the melt than in the UOC source (Nb/Ta = 16.08). Given the uncertainties of these experimental Kd values, with $D_{Nb/Ta}>1.5$, the melts would have Nb/Ta ~ 11, close to the model BCC value of 11.43.

3.1.3.2. The origin of weak negative Eu and Sr anomalies in the continental crust. Likewise, the weak negative Eu and Sr anomalies in the BCC results from plagioclase control during amphibolite melting. While $Kd^{2Sr/(Pr+Nd)}_{Plag}=11.2$ and $Kd^{2Eu/(Sm+Gd)}_{Plag}=17.8$, because there is only ~29.2% plagioclase in the UOC source, $D^{2Sr/(Pr+Nd)}=1.038$ and $D^{2Eu/(Sm+Gd)}=1.209$ (Table 1). These small, but greater than unity values readily explain Eu/Eu* drops from 0.963 in the UOC to 0.803–0.817 in model melts (Fig. 7b), and Sr/Sr* from 1.00 in the OUC to 0.955–0.967 in model melts (Fig. 7b).

3.1.4. The origin of excess Nb, Ta, Ti, Eu and Sr in the MORB mantle

Niu and Batiza (1997) recognized $D^{Nb}\approx D^{Th}<D^{Ta}\approx D^{U}$ and $D^{Ti}\approx D^{Sm}$ in oceanic basalts, and showed $[Nb/Th]_{PM}>1$ and $[Ta/U]_{PM}>1$ of all MORB samples and average OIB that complements the BCC with $[Nb/Th]_{PM}<1$ and $[Ta/U]_{PM}<1$ with respect to the primitive mantle values of unity in $[Nb/Th]_{PM}$ vs. $[Ta/U]_{PM}$ space (see Fig. 5 of Niu and Batiza, 1997), as shown in Table 1. In fact, it is also true that $[Ti/Sm]_{PM}>1$ (~1.111) in primitive MORB melt (see Table 1), which complements $[Ti/Sm]_{PM}<1$ (~0.368) in the BCC (Table 1). All this is consistent with the above calculations that while $D^{Nb}\approx D^{Th}$, $D^{Ta}\approx D^{U}$ and $D^{Ti}\approx D^{Sm}$ during mantle melting for MORB, Nb is much more compatible than Th ($D_{Nb/Th}>40$), Ta is much more compatible than U ($D_{Ta/U}>50$) and Ti is more compatible than Sm ($D_{Ti/Sm}>3.4$) during syncollisional partial melting of amphibolite of MORB protolith. The melting residue thus must have $[Nb/Th]_{PM}>1$, $[Ta/U]_{PM}>1$ and $[Ti/Sm]_{PM}>1$ as reflected by $[Nb/Th]_{MORB13}\approx 2.061$, $[Ta/U]_{MORB13}\approx 1.395$ and $[Ti/Sm]_{MORB13}\approx 1.111$ (Table 1).

Likewise, in the absence of plagioclase involvement during the major mantle melting events for MORB in the spinel peridotite stability field (so is melting, if any, in the garnet peridotite stability field), Sr and Eu cannot fractionate from other otherwise similarly incompatible elements (see Fig. 5a), but $D^{2Sr/(Pr+Nd)}=1.038$ and $D^{2Eu/(Sm+Gd)}=1.209$ during syncollisional partial melting of amphibolite of MORB protolith indicates the presence of excess Eu (Eu/Eu*>1) and Sr (Sr/Sr*>1) in the melting residue.

We infer that the melting residue of amphibolite of UOC protolith is most likely amphibole bearing mafic granulite (e.g., clinopyroxene-orthopyroxene-plagioclase-hornblende-rutile/other oxides) with excess Nb, Ta, Ti, Eu and Sr. As elaborated above, this residue, which is on the top of the continuing underthrusting oceanic lithosphere, will turn into "SiO_2-undersaturated" eclogite (not the same as "removal of free silica during subduction" (Kogiso and Hirschmann, 2006)) and continue to descend into the convective mantle, carrying the inherited geochemical signatures (i.e., excess Sr, Eu, Nb, Ta and Ti).

It is conceptually important to note that compositionally the bulk ocean crust is too depleted and melting of only the UOC (i.e., lavas and feeder dikes) can produce the observed andesitic melt as juvenile material contributing to the growing continental crust mass (Fig. 7). Therefore, while this residue is undepleted or less depleted in terms of major elements relative to mantle peridotite, it is highly depleted in incompatible elements. Hence, in contrast to the popular perception (i.e., Hofmann and White, 1982; Sobolev et al., 2007), recycling of such syncollisional magmatism modified ocean crust (so is recycled ocean crust through active subduction) in the mantle source region cannot produce incompatible element-enriched melt required to explain the enriched characters of ocean island basalts and E-MORB (Niu et al., 2002a; Niu and O'Hara, 2003; Prytulak and Elliott, 2007; Pilet et al., 2008). However, re-mixing of this residual lithology back into the mantle peridotite over much of Earth's history will inevitably imprint the peridotitic mantle with the overall depleted (vs. enriched) geochemical signatures as well as relative enrichments of Nb (vs. Th), Ta (vs. U) and Ti (vs. Sm) (Niu and Batiza, 1997; Niu et al., 1999), and Sr (vs. Pr and Nd) and Eu (vs. Sm and Gd) as we show here (Fig. 4).

3.1.5. Summary on the continental crust growth

Any successful model for continental crust growth must be able to effectively explain key observations. On this basis, we advocate that "continental collision zones (vs. active subduction zones) are primary sites for net continental crust growth" (Niu et al., 2007; Mo et al., 2008). To clarify our preference of this new concept over the standard "island arc" model, Table 2 compares the efficacies of the two models in explaining key observations, in which we do not wish to discuss when and how the proto-type continental crust may form, but how the juvenile continental crustal materials form, how these materials may be preserved to maintain continental crust growth over Earth's

Table 2
Comparison of standard "island arc model" with "collision zone model" for net continental crust growth.

	Island-arc model (Prevailing/standard model)	Collision-zone model (Our preferred hypothesis)
Magma source	Mantle wedge peridotite with subducting slab components	Amphibolite of upper ocean crust of MORB composition
"Primary" melt composition	Basaltic	Andesitic
Additional processes	Unknown processes required to remove the more mafic/ultramafic cumulate into the mantle	No, the melting residue that is more mafic/ultramafic is already in the mantle
Compositional match to continental crust	Very poor	Nearly perfect
Mantle isotopic signature	Yes	Yes
Explanation for relative Nb–Ta–Ti depletion	Yes	Yes
Explanation for relative Th, U, K, LREE enrichment	Yes, but poor	Yes, and excellent
Explanation for weak Sr depletion with respect to Pr and Nd	No, variably high Sr excesses	Yes
Explanation for weak Eu depletion with respect to Sm and Gd	No	Yes
Strong sub-chondritic Nb/Ta ratio	No	Yes
Excess Sr and Eu in melting residue	No	Yes
Excess Nb and Ta in melting residue	Unknown (Yes, in the subducting ocean crust)	Yes
Net juvenile crust addition – 1.	No, mass-balanced by subduction erosion and sediment recycling at present, and likely in the entire Phanerozoic	Yes, preserved in the continental collision zones such as in the southern Tibet as syncollisional andesite and massive granitoid batholiths
Net juvenile crust addition – 2.	No, isolated island arcs moving away from existing continents	Yes, collision can also bring isolated intra-oceanic arcs and oceanic plateaus to the continental masses

history (see Condie, 2005), or at least in the Phanerozoic, and their contributions to the present-day BCC composition.

It is obvious from Table 2 that the continental collision zone model is superior in many aspects. We also need to emphasizes that recognition of model age "spikes" (e.g., McCulloch and Bennett, 1994; Condie, 1998, 2000) preserved in the geologic record suggests that pulses of mantle derived melts, perhaps in the form of "mantle plumes" as a result of "super mantle avalanche events" (e.g., oceanic plateaus and continental flood basalts), may also have contributed episodically to the continental crust mass (Stein and Hofmann, 1994; Abbott and Mooney, 1995; Abbott et al., 1997; Polat et al., 1998; Albarède, 1998; Condie, 2000; Niu et al., 2003; Kerr, 2003; Kemp et al., 2006; Hawkesworth and Kemp, 2006; Parman, 2007; Pearson et al., 2007). Furthermore, if oceanic plateaus are indeed important for continental growth (e.g., Abbott et al., 1997), continental collision remains essential for crustal mass preservation (Niu et al., 2003). Our work in progress suggests that, instead of "super mantle avalanche events", the episodic crustal growth peaks may in fact be associated with continental collisions towards the aggregation of supercontinents. For example, the vast Greater Tibetan Plateau is a geological amalgamation formed by several continental collision events since the Early Paleozoic with suture zones and associated syncollisional granitoid batholiths progressively younger towards south (450 Ma, 420 Ma, 240 Ma, 120 Ma and 55 Ma; Pan et al., 2004) with the youngest being associated with the India–Asia collision (Niu et al., 2007; Mo et al., 2008). All these syncolissional granitoid batholiths are net addition of juvenile materials to the continental crust mass. That is, it is the continental collision that produces and preserves the juvenile crustal material, and hence maintains net continental growth.

3.2. On the chemical structure of the oceanic upper mantle

We have shown some important chemical properties of the DMM such as excess Sr and Eu (also excess Nb, Ta and Ti) that have been unrecognized previously. The question is how much remains unknown about the DMM and whether the widely accepted DMM conjecture is consistent with all the observations. In this section, we review the issue and offer our new perspectives.

It is widely accepted that the DMM lies in the uppermost asthenosphere with less depleted or enriched dikes or veins randomly distributed in the dominantly depleted peridotitic matrix. One of the debates has been the size of the DMM. There have been two recent estimates. Workman and Hart (2005) suggest that the DMM represents at least 30% the mass of the bulk silicate Earth, which is approximately the upper >~800 km of the mantle. On the other hand, Donnelly et al. (2004) suggest that the DMM source is similar to the upper mantle, which is about ~25% the mass of the bulk silicate Earth. Considering the many unknowns and model assumptions plus the fact that the two approaches are entirely different, the two estimates are encouragingly similar. By assuming the traditional view that the DMM indeed lies in the uppermost asthenospheric mantle, we can carry out some exercise by taking a different approach following our recognition of excess Sr and Eu in the DMM and our preferred interpretation that these excesses complement the corresponding Sr and Eu deficiencies in the BCC. We examine what possible DMM source compositions (in terms of REE+Sr) may melt to produce MORB13 (see Figs. 7 and 8). Despite the uncertainties of all sort, we could conclude that the DMM occupies the upper >~680 km or >~26% the mass of the bulk silicate Earth. However, we must emphasize that while such exercise is conceptually interesting, the mantle is unlikely to be of simple two layers with the undepleted or even enriched mass residing in the deep mantle. Furthermore, the DMM may not lie in the uppermost asthenospheric mantle (see below).

3.2.1. More about MORB13

In order to properly estimate the mass of the DMM, the first step is to establish a robust composition of "primary" MORB melt necessary to evaluate the DMM source composition. The MORB13 is thus far the most robust estimate of the depleted and most primitive MORB melt (see details in caption to Fig. 7a).

3.2.2. The composition of the DMM

To estimate the composition of the DMM is conceptually straightforward, but is not so in practice without many assumptions. Using MORB13 to infer the DMM composition requires independent knowledge about the style of melting and melt extraction, the extent of melting and relevant partition coefficients. Nevertheless, we can carry out some simple exercises to place certain constraints. We assume decompression melting in the spinel peridotite stability field by using the polybaric incongruent melting relationship of the form 0.466 Cpx + 0.652 Opx + 0.049 Spl = 0.167Ol + 1.000 Melt (Niu, 1997), where the coefficients determine the effective bulk distribution coefficients P_i, and the initial modes of 0.513Ol, 0.341Opx, 0.131Cpx and 0.015spinel (Niu, 1997) determine the initial bulk distribution coefficients D_i. We use experimentally determined Kd's compiled by Niu et al. (1996; Table 5) (see Fig. 5a). By using the standard non-modal batch and non-modal accumulate fractional melting models (see caption to Fig. 8), we have obtained possible DMM source

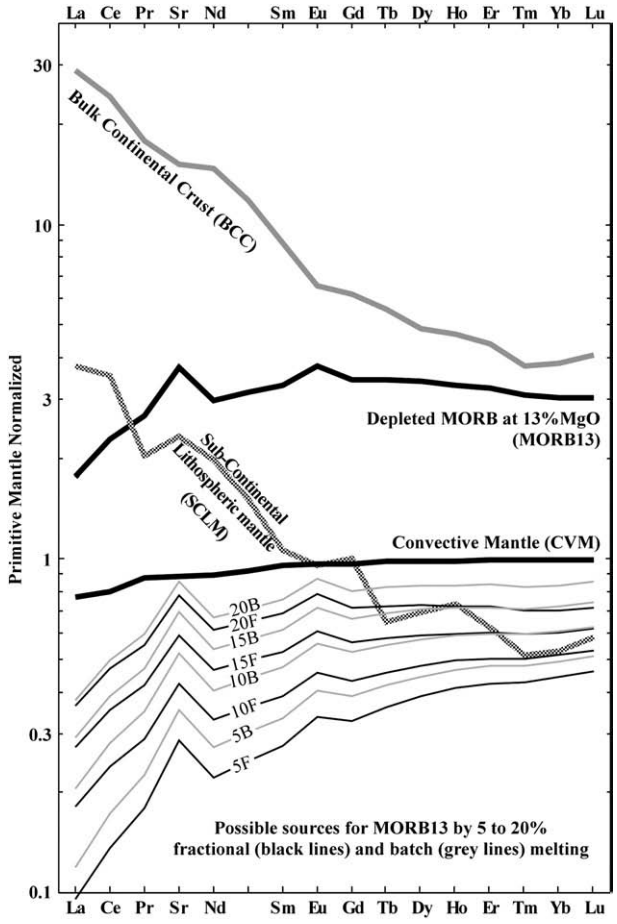

Fig. 8. Primitive mantle (PM) normalized REE+Sr diagram for the BCC composition (Rudnick and Gao, 2003), average composition of sub-continental lithospheric mantle (SCLM; McDonough, 1990), MORB13 (see Fig. 7), model composition of convective mantle (CVM; see below), and calculated possible model DMM compositions required to produce the MORB13 (see below). By using the polybaric incongruent melting relationship of the form 0.466 Cpx + 0.652 Opx + 0.049 Spl = 0.167Ol + 1.000 Melt (Niu, 1997), MORB13 can be produced by non-modal batch $X^i_{Source} = X^i_{MORB13}(D_j{}^1 + F(1\text{-}P_j{}^i))$ and fractional $[X^i_{Source} = X^i_{MORB13}/(1/F(1\text{-}(1\text{-}P^i_jF/D^i_j)^{1/P_j i}))]$ melting from possible source compositions by 5 to 20% batch (labeled as 5B, 10B, 15B, 20B) or fractional (labeled as 5F, 10F, 15F, 20F) melting. In these equations, F, the extent of melting; D, bulk distribution coefficient of element i (REEs and Sr) for mineral j with initial modes of 0.513Ol, 0.341Opx, 0.131Cpx and 0.015spinel (Niu, 1997); and P, bulk distribution coefficient of element i (REEs and Sr) for mineral j with non-modal melting modes of −0.167Ol, 0.466Cpx, 0.652Opx and 0.049Spinel (Niu, 1997). Relevant individual partition coefficients are given in Fig. 5a (also Table 5 of Niu et al., 1996). Physically, the CVM [$3.911*10^{27}$g] = PM [$4.034*10^{27}$g] (Jacobsen and Wasserburg, 1979) − BCC [$2.256*10^{25}$g] (Jacobsen and Wasserburg, 1979) − SCLM [$1.0027*10^{26}$g] (Pearson and Nowell, 2002). We use this information and compositions of the PM (Sun and McDonough, 1989), BCC (Rudnick and Gao, 2003) and SCLM (McDonough, 1990) to obtain the model composition of the CVM (i.e., X^i_{CVM} for element i).

compositions that can all potentially produce MORB13 by varying extents (5%, 10%, 15% and 20%) of batch (5B, 10B, 15B and 20B) and fractional (5F, 10F, 15F and 20F) melting (Fig. 8).

Obviously, MORB13 can be produced by high extents of melting from a less depleted source (e.g., 20F or B20) or by low extents of melting from a more depleted source (e.g., 5F or B5). As a result, a large DMM volume is obtained if the DMM source is less depleted (e.g., 20F; Fig. 8) or a smaller DMM volume is obtained if the DMM source is highly depleted (e.g., 5F; Fig. 8) because the composition of MORB13 is fixed, but the extent of melting is unknown. Hence, there is no unique solution. The argument can then be made by assuming that the extent of melting for MORB is known, in which case the DMM composition can be constrained (see Fig. 8). However, there is no consensus on the extent of mantle melting for MORB although it is clear that the extent of melting increases with increasing spreading rate (Niu and Hékinian, 1997a) and may also increase with decreasing ridge axial depth due to speculated mantle temperature variation (Klein and Langmuir, 1987) or due actually to fertile mantle density controlled amplitude and rate of mantle upwelling (Niu and O'Hara, 2008). Low extent of melting (~6%) is favoured based solely on MORB geochemistry modelling (Asimow et al., 2004; Workman and Hart, 2005; also see below), but Niu (1997) suggested higher extent of melting (~15%) as revealed from abyssal peridotite studies and based on the simple physical argument that low extents of melting face difficulties in generating the 6–7 km thick ocean crust unless the ocean crust is much thinner (see below).

3.2.3. The volume of the DMM

It is conceptually appropriate to estimate mass fraction of the DMM not with respect to the primitive mantle, but with respect to the bulk convective mantle (CVM), which includes oceanic lithosphere (crust+mantle lithosphere), and whose total mass and compositions can be readily calculated using existing data (see caption to Fig. 8).

Fig. 9a shows mass fractions of the mantle from 80 km depth (assumed to be the mean thickness of the "continental lithosphere" across the globe) downwards as a function of depth. The mass fraction of the DMM and its deep bound labelled with 5F, 10F, 15F and 20F are derived from the calculated MORB13 sources using the accumulated fractional melting models in Fig. 8 (see caption to Fig. 9a). These calculations are only meant to illustrate the concept and cannot be taken as true or correct because of the assumptions and because it also depends on which element is used. In these calculations, we use La, the most incompatible REE and the mass balance equation (using model DMM composition F10 as an example): $X^{La}_{CVM} = f^{F10}_{DMM}X^{La,F10}_{DMM} + (1\text{-}f^{F10}_{DMM})X^{La}_{PM}$. That is, the bulk CVM is considered to consist of two parts, the upper DMM with mass fraction of f^{F10}_{DMM} and the rest deeper undepleted mantle with primitive mantle composition for conceptual clarity.

Fig. 9b plots the deep bound of calculated DMM with compositions represented by 5F, 10F, 15F and 20F (Figs. 8 and 9a) against excess Eu and Sr masses calculated from the positive anomalies of the corresponding model DMM sources (Fig. 8). For comparison, the masses of missing Eu and Sr in the BCC calculated from the negative Eu and Sr anomalies in the BCC are also plotted. Obviously, the model DMM sources all have much more excess Eu and Sr than needed to account for the missing Eu and Sr in the BCC. A DMM source more depleted than 5F (Fig. 8) can balance the crust–mantle Eu and Sr budgets. This would place the deep bound of the DMM to 621 km in terms of excess of Eu and to 585 km in terms of excess Sr by using 3 rd order polynomial extrapolations (curves) defined by these model DMM sources (Fig. 9a). If the more incompatible element such as Nb (vs. La) is used, the DMM mass fractions would be shifted to higher values (i.e., greater depths for the deep bound of the DMM) but the masses of the excess Eu and Sr in Fig. 9b will not change.

It is important to note the apparent problem common to all geochemical models of this kind. Fig. 9b shows that the DMM source with excess Sr and Eu required to mass-balance the Sr- and Eu-deficient BCC becomes too depleted (the intercepts of the model DMM curves with the horizontal BCC lines) to produce MORB13 by our melting models described above (Fig. 8) unless the average extent of melting is ~1%, which is unlikely. It is possible that our melting models are too simplistic and the compound uncertainties from all the assumptions in our model calculations may contribute to the discrepancies.

However, the most sensitive uncertainties in these calculations are in fact Eu and Sr values of the PM used for normalization and Eu and Sr abundances in the BCC. The Eu value in the PM (0.168 ppm; Sun and McDonough, 1989) is probably reasonable because it is constrained by other REEs. However, the PM Sr value (21.1 ppm) may be not. For the most primitive MORB melt with MgO = 10 wt.%, Sr/Sr* = 1.3293 (Fig. 4b), but this positive anomaly would become 1.1687 comparable

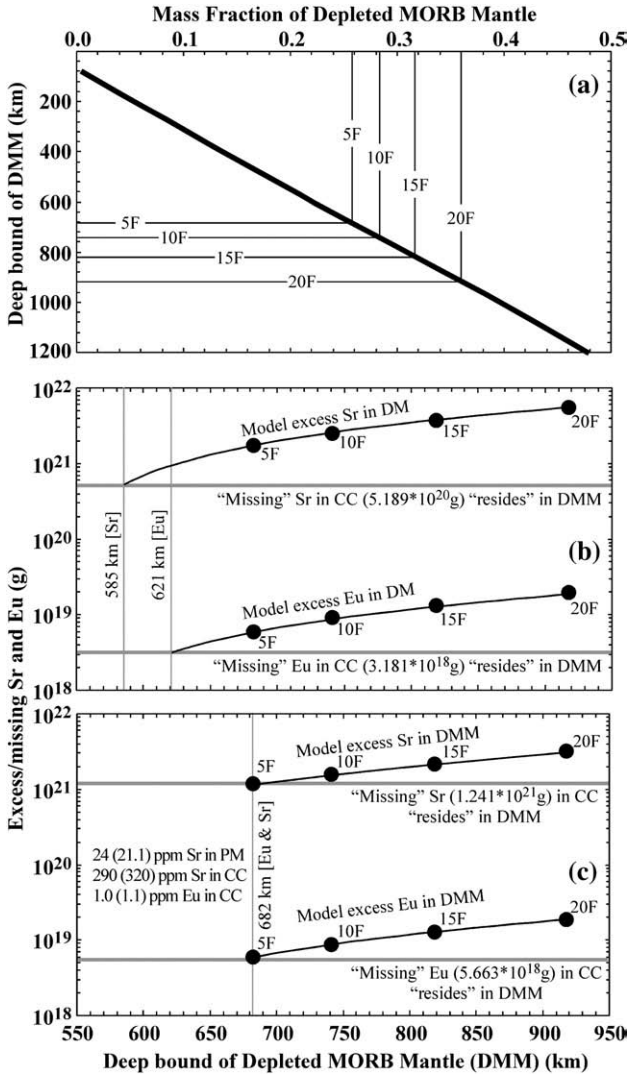

Fig. 9. (a) The thick line represents mass fraction of convective mantle (CVM) as a function of depth from 80 km downward derived from the PREM (Dziewonski and Anderson, 1981), which is apparently linear in the section chosen (i.e., <1200 km depth), but is best described by the polynomial fit ($y = 1308.9x^3 + 1079.4x^2 + 2590x + 65.135$, where y is mass fraction and x is depth in km) for the entire mantle. Mass fraction of the depleted mantle is calculated from PM-normalized La values of possible sources F5, F10, F15 and F20 for MORB13, e.g., $f^{F10}_{DMM} = (X^i_{CVM} - 1)/(X^{i,F10}_{DMM} - 1)$. Obviously, such calculations are poorly constrained because using different elements will result in different f_{DMM} values, which are greater when the more incompatible elements are used. For conceptual clarify, we use La, the most incompatible REE. As expected, the more depleted the DMM is (e.g., F5 is more depleted than F10 in Fig. 8), the smaller the DMM volume is as constrained by MORB13. This exercise suggests that the volume of the DMM is the entire upper mantle, or perhaps even includes uppermost portions of the lower mantle. (b) Positive Sr and Eu anomalies in model DMM sources (see Fig. 8) should be mass-balanced by the missing Sr and Eu in the BCC. However, the Sr and Eu excess in model DMM compositions is much higher than needed to balance the missing Sr ($5.189*10^{20}$g) and Eu ($3.181*10^{18}$g) in the BCC. In order to explain the Sr and Eu complementarity, it requires that the DMM be more depleted than 20F, 15F, 10F and even 5F (see Fig. 8). That is, the match is where the "DMM-excess" curves and the "BCC-missing" horizontal lines intersect. Third order polynomial extrapolations of model DMM source compositions 20F, 15F, 10F and 5F give deep bound DMM depths of 585 km using Sr and 621 km using Eu, respectively. The two values are essentially the same, i.e., 600 ± 20 km. That is, the missing Sr and Eu in the continental crust may be hosted in the upper 600 km DMM. However, this implies that the DMM is even more depleted than 5F unless the extent of melting is ~1%. (c) Revision of input parameters within reasonable range such as the PM Sr value of 24 ppm (vs. 21.1) and Sr and Eu deficiency of ~10% more than the BCC leads to different results, i.e., the DMM could occupy the upper most ~680 km of the CVM (see text for details).

to Eu/Eu* = 0.1205 if we choose a PM Sr value of 24 ppm. REE abundances of the BCC is largely budgeted by the upper crust which is better constrained with a huge negative Eu anomaly (Eu/Eu* = 0.706) (Fig. 2b). If the deep crust Eu is overestimated, and if the BCC Eu is thus overestimated by 10%, i.e., if we use bulk BCC Eu = 1.0 ppm instead of 1.1 ppm (Rudnick and Gao, 2003), then there would be more missing Eu in the BCC that resides in the DMM. For the same reasoning, we use BCC Sr = 290 ppm, about 90% of 320 ppm (Rudnick and Gao, 2003). All these re-adjustments lead to a very different result (Fig. 9c), which increases BCC Sr deficiency by 2.3 times, and CC Eu deficiency by 1.8 times. Therefore, the depleted DMM source F5 can produce MORB13 as well as REE-Sr budget between the BCC and DMM that occupies the upper ~680 km (or ~26% the mass) of the convective mantle. This DMM mass/volume estimate is geochemically sensible because the adjusted abundances of Eu (for the BCC) and Sr (for the PM and BCC) are within ~10% uncertainty range. Nevertheless, this estimate may actually be the lower limit as it is derived from the most depleted MORB (Figs. 7 and 8) without considering enriched heterogeneities hosted in the DMM accounting for E-type MORB. However, the enriched materials may not be abundant, but randomly distributed in the depleted peridotite matrix (Niu et al., 1999, 2002a). Perhaps, E-type MORB may have different origins (see below).

Our estimated DMM mass/volume on the basis of Sr and Eu anomalies is similar to the estimates by Donnelly et al. (2004) and Workman and Hart (2005) using different approaches, but what is in common in all these estimates is the implication that MORB forms by ~6% near fractional melting. While the 6% melting is consistent with MORB geochemistry-based arguments, such low extent of melting is inconsistent with estimates from abyssal peridotites (Niu, 1997) and is too low to form the required 6–7 km thick ocean crust (see below).

3.2.4. Constraints, caveats and alternatives

3.2.4.1. Constraints. In order to model the average composition of the DMM and its volume, the first step is to derive the composition of the most primitive MORB melt. The MORB melt composition at 10% MgO or "primary MORB melt" at 13% MgO we obtained, MORB13, is so far the most robust estimate of such a melt with minimal, if any at all, assumption (Fig. 7). Any model DMM composition must be able to produce this "primary" melt. The recognition of positive Eu and Sr anomalies in primitive MORB melts (Fig. 4), and thus in the "primary" MORB melt with 13% MgO (Fig. 8) points to excess Eu and Sr in the DMM, which, together with the Nb, Ta and Ti excesses in the DMM (Niu and Batiza, 1997) (also see Table 1), sheds new light on the origin of the DMM. This, plus the huge negative Nb and Ta anomalies, moderate negative Ti anomaly and weak yet significant negative Eu and Sr anomalies in the BCC (Rudnick and Gao, 2003), corroborates the notion that the DMM complements the BCC. Hence, any model for the composition and volume of the DMM must be consistent with the constraints offered by the Nb–Ta–Ti–Sr–Eu complementarity between the DMM and BCC although uncertainties on the primitive mantle value for Sr and uncertainties on the size of the negative Eu, Sr, Nb and Ta anomalies in the BCC can affect the model DMM composition (i.e., how depleted it may be) and hence its volume (see above). The above statements and arguments are valid if the primitive mantle (or bulk silicate Earth) has no Eu, Sr, Nb, Ta and Ti anomalies with respect to bulk earth composition that is strictly chondritic (see Fig. 1).

3.2.4.2. Caveats. The apparent consistency among different estimates (Donnelley et al., 2004; Workman and Hart, 2005) and exercises of this study on the DMM volume requires the mean extent of MORB mantle melting to be ~6%, which is considered to be robust because it is also consistent with another independent study (Asimow et al., 2004). The validity of this geochemically robust estimate in extent of melting must be tested against some straightforward physical arguments. Following the argument by Phipps Morgan (1987), Niu (1997) showed that for a perfect passive upwelling mantle, melt produced in the mantle farther than ~180, 90, 60 and 45 km beneath both plates must transport laterally towards the ridge axis to form the

~6 km thick crust inferred from seismic data (White et al., 1992) if the average extent of melting is 5%, 10%, 15% and 20%, respectively. Niu (1997) suggested on the basis of abyssal peridotite data an average of 15% melting for MORB, which requires that melt form and transport to the ridge axis from a broad zone of >120 km (>60 km on each side of the ridge) across the ridge. This problem that has never been resolved (see Forsyth, 1992) has disappeared in the more recent literature. The problem persists and it remains enigmatic how melts formed >150 km from each side of the ridge (for 6% melting) migrate towards the ridge axis to form the ~6 km thick crust. It is even more problematic whether the sub-ridge mantle >150 km away from the ridge can melt at all by decompression that may have restricted rate and amplitude of upwelling, in particular beneath slow-spreading ridges. Therefore, the apparently consistent models in terms of geochemistry must be tested against physical likelihood. It remains possible that the magmatic ocean crust may indeed be much thinner than inferred from seismic data (Hess, 1962; Christensen, 1972; Niu, 1997; Niu and O'Hara, 2008).

The notion that the DMM lies in the uppermost portion of the asthenosphere with the deep mantle undepleted or perhaps even enriched is based on some logical reasoning. The mostly passive upwelling beneath ocean ridges suggests that MORB sample the shallowest mantle. The overall incompatible element depleted composition of MORB further suggests that the shallowest mantle is depleted. The first-order compositional complementarity between the continental crust and the shallowest mantle inferred from MORB is hinted at a genetic relationship, thus supporting the idea further that the DMM lies in the uppermost portion of the asthenospheric mantle. Yet, exactly how depleted it is depends on its size if the continental crust is indeed the "culprit" for the depletion of the DMM, which is the very reason we carried out our exercise above. However, this apparently logical reasoning may not be correct. The seismic observation that some subducting oceanic lithosphere can indeed penetrate the 660-D (e.g., van der Hilst et al., 1997; Grand et al., 1997) into the lower mantle requires that materials from the lower mantle rise to the upper mantle to balance the mass. Hence, such large scale mass exchange over a significant portion of Earth's history may invalidate our perception on the size and location of the DMM. Both depleted and enriched materials must exist throughout the convective mantle. But if so, why do MORB sample the DMM composition?

3.2.4.3. Alternatives. Fig. 10a illustrates the familiar concept that oceanic lithosphere grows with time through basal accretion of the seismic low velocity zone (LVZ) material (red arrows) for ~70 million years before reaching its full thickness. The presence of small amount of melt may in fact be required by and characterize the LVZ (Lambert and Wyllie, 1968, 1970; Green, 1971; Green and Liebermann, 1976;

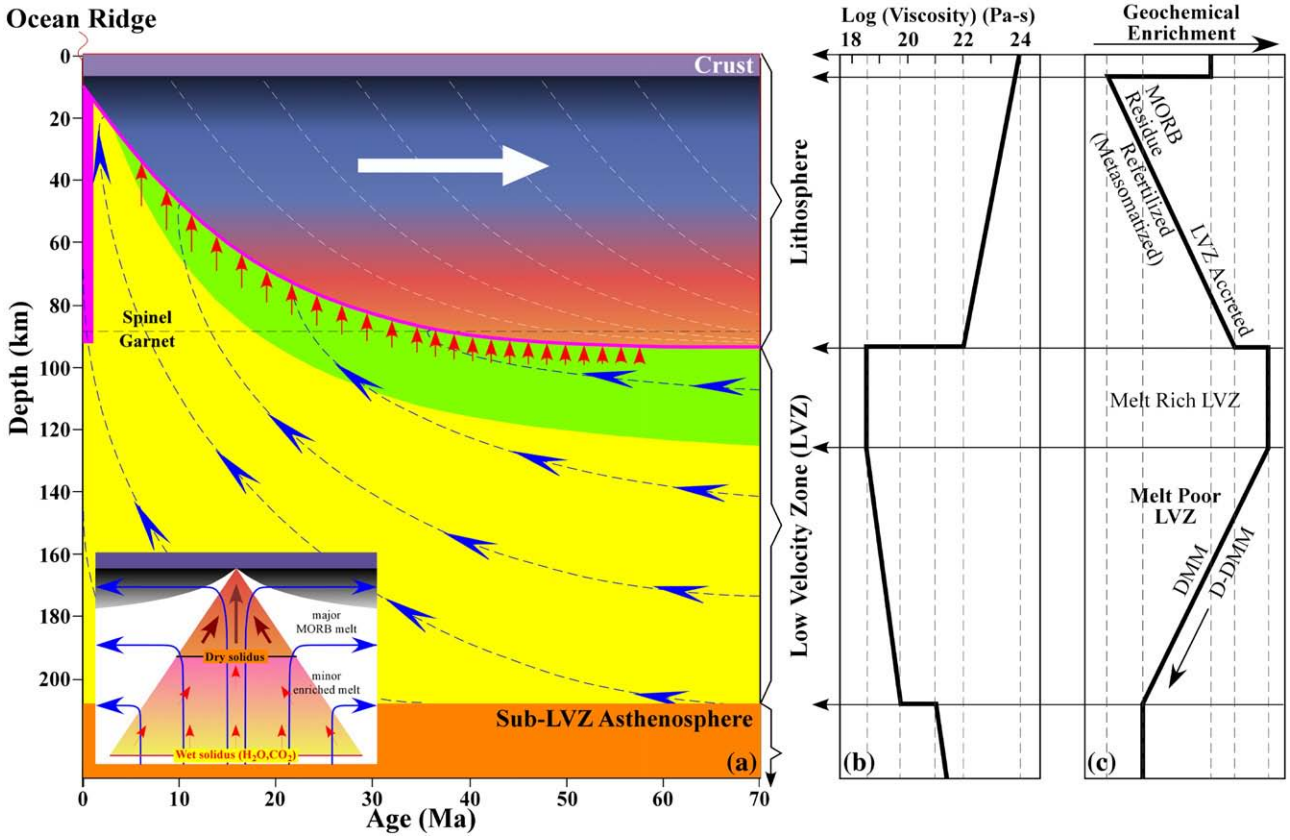

Fig. 10. (a) Oceanic lithosphere grows with time through basal accretion of the LVZ material (red arrows) for ~70 million years before reaching its full thickness of ~95 km in terms of the plate model by Stein and Stein (1992). The thick purple curve is the present-day interface between the forming lithosphere and the LVZ, which is a natural solidus marking the petrologic transition from solid pargasite-bearing peridotite to peridotite containing a small melt fraction (Lambert and Wyllie, 1968, 1970;Green, 1971; Green and Liebermann, 1976). The thin white dashed curves indicate where this interface was in the past, illustrating the continuing lithosphere growth with time as the plate ages. The small melt fraction in the LVZ would be enriched in volatiles (e.g., H_2O, CO_2) and incompatible elements (Niu et al., 2002a; Niu and O'Hara, 2003). As the melt is buoyant at such depth range, it tends to concentrate towards the top of the LVZ as indicated by the green band. In the process of the lithosphere growth, the uppermost LVZ material forms spinel/garnet lherzolite with pargasite amphibole (Green and Liebermann, 1976) as newly accreted lithosphere. Trapped low-degree melts of LVZ origin collect, ascend, and metasomatize the ambient peridotite. Because it takes ~70 million years for the lithosphere to reach its full thickness, the metasomatism continues during this time. The key point here is that what is supplied to the ridge for MORB is predominantly the depleted deep portions of the LVZ, explaining the generally depleted MORB composition, and some alkali-rich basalts on off-ridge seamounts. This offers a simple alternative to the common perception that enriched component in some MORB necessarily comes directly from low-degree melt formed at great depth when upwelling mantle intersects the wet solidus (see the inset). (b) A schematic viscosity profile as a function of depth beneath the mature oceanic lithosphere. (c) Schematic illustration of geochemical enrichment in terms of volatile contents and progressively more incompatible elements (e.g., La/Sm, Rb/Sr, Nb/Zr). (For interpretation of the references to colour in this figure legend, the reader is referred to the web version of this article.)

Anderson, 1995; Niu and O'Hara, 2003). This melt would be enriched in volatiles (e.g., H_2O, CO_2) and incompatible elements (Niu et al., 2002a; Niu and O'Hara, 2003). As the melt is buoyant at such depth range, it tends to concentrate towards the top of the LVZ as indicated by the green band. In the process of the lithosphere growth, the uppermost LVZ material forms spinel/garnet lherzolite with pargasite amphibole (Green and Liebermann, 1976) as newly accreted lithosphere. Trapped low-degree melts of LVZ origin collect and ascend, crystallizing liquidus minerals added to the ambient peridotite (modal metasomatism), and leaving behind veins of garnet-pyroxenite, hornblende-pyroxenite and hornblendite (Pilet et al., 2008) before being finally absorbed in the ambient minerals (cryptic metasomatism) (O'Reilly and Griffin, 1988). Because it takes ~70 million years for the lithosphere to reach its full thickness, such metasomatism continues during this time. This is equivalent to a distance of 700 km from the ridge if the plate moves slowly at 10 mm/year and of 4200 km if the plate moves fast at 60 mm/year (Niu, 2008). Hence, the oceanic lithosphere is a huge geochemical reservoir enriched in volatiles and incompatible elements despite its upper sections being MORB melting residues (Fig. 10c). Recycling of such metasomatized lithosphere into the deep mantle over much of Earth's history will cause mantle compositional heterogeneities on all scales, responsible for the enriched characters of ocean island basalts and E-type MORB (Niu et al., 2002a; Niu and O'Hara, 2003; Niu, 2008).

While ocean ridges are mostly passive features in the context of plate tectonics, they play an active and controlling role in dictating sub-lithospheric mantle flow. This is simply because of the fact that the LVZ beneath ocean ridges represents regions of lowest pressure in the entire asthenosphere that drives ridge-ward asthenospheric flow, i.e., ridge suction. The ridge suction results from the material needs to form the ocean crust at the ridge and much of the mantle lithosphere in the vicinity of the ridge (Niu and Hékinian, 2004). Because the mantle viscosity increases exponentially with depth in the sub-LVZ asthenosphere (Fig. 10b; e.g., Phipps Morgan et al., 1995), the LVZ (also low-viscosity-zone or lvz) materials must move laterally to supply the ridge, leading to the inevitable decoupling between the moving plates and the subjacent LVZ with the degree of decoupling increases with increasing plate spreading rate (Niu and Hékinian, 2004; Niu, 2005).

The key point here is that the ridge suction force (or material flux) is significant and what is supplied to the ridge for MORB as a result of the "ridge suction" is predominantly the depleted (volatile and incompatible element poor) deep portions of the LVZ (yellow; Fig. 10a,c), explaining the generally depleted MORB composition, and some alkali-rich basalts on off-axis seamounts (Batiza and Vanko, 1984; Batiza et al., 1989, 1990; Zindler et al., 1984; Niu and Batiza, 1997). The E-type MORB, which are compositional mix of normal MORB with alkali-rich components seen in off-ridge seamount lavas (Batiza, 1982; Batiza et al., 1989), are mostly caused by contributions from the entrained LVZ melt (the green) as a result of shallow level lithospheric adjustment (e.g., localities of ridge jumps, offsets, transform effects, lithospheric cracks etc.). This offers a conceptually simple and viable alternative to the common perception that enriched component in E-type MORB necessarily comes from low-degree melt formed at great depths when upwelling mantle intersects the wet solidus (see inset in Fig. 10a; Langmuir et al., 1992; Asimow and Langmuir, 2003). The latter process is possible (Niu et al., 1996), but its physical difficulty lies in the fact that such low-degree melt, if produced at all, will be diluted by the main stream mantle flow and will not surface as distinct E-type MORB. This analysis offers a new perspective on the compositional structure of the uppermost ~200 km of the oceanic mantle (Fig. 10c) that differs from the widely perceived concept of the DMM. The DMM, while compositionally complementing the BCC, may have a rather complex history involving conceptually simple but physically complex processes as we perceive in Fig. 10.

We emphasize that the dynamics of the LVZ may in fact play a critical role in plate tectonics, intraplate magmatism (Niu, 2008) and crustal mantle differentiation. For example, the LVZ may serve as the "factory" where compositionally heterogeneous asthenospheric mantle is differentiated into the melt-rich layer (green band in Fig. 10a) towards the top to metasomatize and accrete the growing oceanic lithosphere (red arrows in Fig. 10a) whereas the deeper "residual" melt-poor portion (yellow in Fig. 10a) become the DMM feeding MORB. While the LVZ is poorly defined beneath the cratonic mantle lithosphere, it must also exist there and explain the metasomatic enrichments observed in subcontinental lithospheric mantle (e.g., O'Reilly and Griffin, 1988; McDonough, 1990). Caution is thus necessary when accepting the interpretation/inference as a well-established fact that the DMM simply occupies the uppermost asthenospheric mantle.

4. Summary

(1) We have recognized in high quality MORB glass data that Eu/Eu* and Sr/Sr* show a correlated variation and both decrease with decreasing MgO, pointing to the effect of plagioclase crystallization.

(2) Primitive MORB melts with MgO>9.5 wt.% (prior to plagioclase crystallization) all have Eu/Eu*>1 and Sr/Sr*>1, indicating that the DMM has excess Eu (Eu/Eu*>1) and Sr (Sr/Sr*>1).

(3) The observation that $D^{Nb}\approx D^{th}$, $D^{Ta}\approx D^{U}$ and $D^{Ti}\approx D^{Sm}$during mantle melting for MORB, yet primitive MORB melts all have $[Nb/Th]_{PM}^{MORB}>1$, $[Ta/U]_{PM}^{MORB}>1$ and $[Ti/Sm]_{PM}^{MORB}>1$ (Niu and Batiza, 1997) indicate that the DMM also has excess Nb (vs. Th), Ta (vs. U) and Ti (vs. Sm).

(4) Our recognition that the excess Eu, Sr, Nb, Ta and Ti in the DMM complement the deficiency of these elements in the BCC offers new insights into the genetic relationship between the two. All the observations consistently favour the hypothesis that continental collision zones are primary sites of net continental crust growth. Partial melting of amphibolite of MORB protolith during continental collision produces andesitic melt that shows remarkable compositional similarity to the BCC (Fig. 8 of Mo et al., 2008). The andesitic melt represents the juvenile crust (both volcanic rocks and granitoids) preserved in the continent. These contrast with the standard "island arc" model that has many more difficulties than certainties.

(5) It is the continental collision towards supercontinent amalgamation (vs. "super mantle avalanche events") that produces and preserves the juvenile crustal material, and hence maintains net continental growth over earth's history.

(6) We have established the thus far the most robust trace element composition of depleted "primary" MORB melt with 13% MgO, which together with the positive Eu and Sr anomalies allow estimation of the composition of the DMM as well as its size following the tradition that the DMM occupies the shallowest asthenospheric mantle. However, this tradition may be in error.

(7) The LVZ may be compositionally stratified with small melt fractions concentrated towards the interface of the growing lithosphere. Such melt fractions are enriched in volatiles and incompatible elements that continue to metasomatize the growing lithosphere before it reaches the full thickness after ~70 Myrs. Hence, the oceanic mantle lithosphere is a huge enriched geochemical reservoir.

(8) Deep portions of the LVZ, which are thus relatively depleted, become the primary source feeding the ridge for MORB. This analysis offers a new perspective on the compositional structure of the uppermost ~200 km of the oceanic mantle that differs from the common perception of the DMM. The DMM, while complementary to the BCC, may not be distributed in space and time as widely perceived and the DMM materials may have a rather complex history involving complex processes.

(9) We emphasize that the dynamics of the LVZ may in fact play a critical role in plate tectonics, intraplate magmatism and crustal mantle differentiation.

(10) Specifically designed and well controlled melting experiments of amphibolites of MORB protolith with and without terrigenous sediments will be important for establishing melting reactions needed for improved petrologic and geochemical modeling we attemp (Table 1 and Fig. 7).

Acknowledgements

It is our great pleasure to contribute to the special volume in honour of Roger Hékinian for his pioneering effort and life-long contributions to seafloor petrology and marine geology research. YN thanks Roger for his support, friendship, encouragement and enjoyable research collaboration over the years. YN also thanks The Leverhulme Trust for a Research Fellowship. Discussion with Kevin Burke, Jon Davidson, Chris Hawkesworth, Al Hofmann, Bob Kay, Charlie Langmuir, Bill McDonough, Xuanxue Mo, Graham Pearson, Terry Plank, Ali Polat, Marcel Regelous, Roberta Rudnick, Peter Wyllie, Youxue Zhang, Zhidan Zhao, Xinhua Zhou and Dicheng Zhu has been useful. We thank Nelson Eby, Fred Frey and an anonymous reviewer for constructive comments that have helped improve the paper.

References

Abbott, D., Mooney, W., 1995. The structural and geochemical evolution of the continental crust support for the oceanic plateau model of continental growth. Review of Geophysics 1991–94, 231–242.
Abbott, D.H., Drury, R., Mooney, W.D., 1997. Continents as lithological icebergs: the importance of buoyant lithospheric roots. Earth and Planetary Science Letters 149, 15–27.
Albarède, F., 1998. The growth of continental crust. Tectonophysics 296, 1–14.
Allègre, C.J., Hart, S.R., Minster, J.-F., 1983. Chemical structure and evolution of the mantle and continents determined by inversion of Nd and Sr isotopic data, I. Theoretical methods. Earth and Planetary Science Letters 66, 177–190.
Anderson, D.L., 1995. Lithosphere, asthenosphere, and perisphere. Reviews of Geophysics 33, 125–149.
Arculus, R.J., 1981. Island arc magmatism in relation to the evolution of the crust and mantle. Tectonophysics. 75, 113–133.
Armstrong, R.L., 1968. A model for the evolution of strontium and lead isotopes in a dynamic earth. Review of Geophysics and Space Physics 6, 175–200.
Asimow, P.D., Langmuir, C.H., 2003. The importance of water to oceanic mantle melting regimes. Nature 421, 815–820.
Asimow, P.D., Dixon, J.E., Langmuir, C.H., 2004. A hudrous melting and fractionation model for mid-ocean ridge basalts: application to the Mid-Atlantic Ridge near Azores. Geochemistry Geophysics Geosystems 5. doi:10.1029/2003GC000568.
Batiza, R., 1982. Abundance distribution and sizes of volcanoes in the Pacific Ocean and implications for the origin of non-hotspot volcanoes. Earth and Planetary Science Letters 60, 196–206.
Batiza, R., Vanko, D.A., 1984. Petrology of young Pacific seamounts. Journal of Geophysical Research 89, 11,235–11,260.
Batiza, R., Smith, T.L., Niu, Y.L., 1989. Geologic and petrologic evolution of seamounts near the EPR based on submersible and camera study. Marine Geophysical Research 11, 169–236 1989.
Batiza, R., Niu, Y.L., Zayac, W.C., 1990. Chemistry of seamounts near the East Pacific Rise: Implications for the geometry of subaxial mantle flow. Geology 18, 1122–1125 1990.
Bédard, J.H., 2006. Trace element partitioning in plagioclase feldspar. Geochimica et Cosmochimica Acta 70, 3717–3742.
Blundy, J.D., Wood, B.J., 1991. Crystal-chemical controls on the partitioning of Sr and Ba between plagioclase feldspar, silicate melts, and hydrothermal solutions. Geochimica et Cosmochimica Acta 55, 193–209.
Brenan, J.M., Shaw, H.F., Ryerson, F.J., Phinney, D.L., 1995. Experimental-determination of trace-element partitioning between pargasite and a synthetic hydrous andesitic melt. Earth and Planetary Science Letters 135, 1–11.
Castillo, P.R., 2006. An overview of adakite petrogenesis. Chinese Science Bulletin 51, 257–268.
Castillo, P.R., Natland, J.H., Niu, Y.L., Lonsdale, P., 1998. Sr, Nd, and Pb isotopic variation along the Pacific ridges from 53 to 56°S: implications for mantle and crustal dynamic processes. Earth and Planetary Science Letters 154, 109–125.
Christensen, N.I., 1972. Abundance of serpentinites in oceanic crust. Journal of Geology 80, 709–719.
Clift, P., Vannucchi, P., 2004. Controls on tectonic accretion versus erosion in subduction zones: implications for the origin and recycling of the continental crust. Review of Geophysics 42, RG2001. doi:10.1029/2003RG000127. 31 pp.
Condie, K.C., 1998. Episodic continental growth and supercontinents: a mantle avalanche connection? Earth and Planetary Science Letters 163, 97–108.
Condie, K.C., 2000. Episodic continental growth models: afterthoughts and extensions. Tectonophysics 322, 153–162.
Condie, K.C., 2005. Earth as an evolving planetary system. Elsevier Academic Press, London. 447 pp.
Davidson, J.P., Arculus, R.J., 2006. The significance of Phanerozoic arc magmatism in generating continental crust. In: Brown, M., Rushmer, T. (Eds.), Evolution and Differentiation of the Continental Crust. Cambridge Press, pp. 135–172.
Defant, M.J., Drummond, M.S., 1990. Derivation of some modern arc magmas by melting of young subducted lithosphere. Nature, 347, 662–665.
Dick, H.J.B., 1989. Abyssal peridotites, very slow spreading ridges and ocean ridge magmatism. Geological Society Special Publication 42, 71–105.
Donnelly, K.E., Goldstein, S.L., Langmuir, C.H., Spiegelman, M., 2004. Origin of enriched ocean ridge basalts and implications for mantle dynamics. Earth and Planetary Science Letters 226, 347–366.
Dostal, J., Dupuy, C., Carron, J.P., Dekerneizon, M.L., Maury, R.C., 1983. Partition-coefficients of trace elements – application to volcanic rocks of St Vincent, West Indies. Geochimica et Cosmochimica Acta 47, 525–533.
Drake, M.J., Weill, D.F., 1975. Partition of Sr, Ba, Ca, Y, Eu^{2+}, Eu^{3+}, and other REE between plagioclase feldspar and magmatic liquid – experimental study. Geochimica et Cosmochimica Acta 39, 689–712.
Dunn, T., Sen, C., 1994. Mineral/matrix partition-coefficients for orthopyroxene, plagioclase, and olivine in basaltic to andesitic systems – a combined analytical and experimental study. Geochimica et Cosmochimica Acta 58, 717–733.
Dziewonski, A.M., Anderson, D.L., 1981. Preliminary reference Earth model. Physics of the Earth and Planetary Interiors 25, 297–356.
Elliott, T., 2003. Tracers of the slab. Geophysical Monograph 238, 23–45.
Foley, S., Tiepolo, M., Vannucci, R., 2002. Growth of early continental crust controlled by melting of amphibolite in subduction zones. Nature 417, 837–840.
Forsyth, D.W., 1992. Geophysical constraints on mantle flow and melt generation beneath mid-ocean ridges. American Geophysical Union Monograph 71, 1–66.
Frey, F.A., Haskin, M.A., Poetz, J.A., Haskin, L.A., 1968. Rare earth abundances in some basic rocks. Journal of Geophysical Research 73, 6085–6098.
Fujimaki, H., Tatsumoto, M., Aoki, K.-I., 1984. Partition coefficients of Hf, Zr, and REE between phenocrysts and groundmasses. Journal of Geophysical Research 89, 662–672.
Gao, S., Zhang, B.-R., Jin, Z.-M., Kern, H., Luo, T.-C., Zhao, Z.-D., 1998. How mafic is the lower continental crust? Earth and Planetary Science Letters 106, 101–117.
Gast, P.W., 1968. Trace element fractionation and the origin of tholeiitic and alkaline magma types. Geochimica et Cosmochimica Acta 32, 1055–1086.
Gill, J.B., 1981. Orogenic Andesites and Plate Tectonics. Springer-Verlag, New York. 390 pp.
Grand, S.P., van der Hilst, R.D., Widiyantoro, S., 1997. Global seismic tomography: a snapshot of convection in the Earth. GSA Today 7, 1–7.
Green, D.H., 1971. Composition of basaltic magmas as indicators of conditions of origin: application to oceanic volcanism. Philosophical Transaction, Royal Society of London A268, 707–725.
Green, D.H., Liebermann, R.C., 1976. Phase equilibria and elastic properties of a Pyrolite model for the oceanic upper mantle. Tectonophysics 32, 61–92.
Hanson, G.N., 1980. Rare earth elements in petrogenetic studies of igneous systems. Annual Review of Earth and Planetary Sciences 8, 371–460.
Hawkesworth, C.J., Kemp, A.I.S., 2006. The differentiation and rates of generation of the continental crust. Chemical Geology 226, 134–143.
Hékinian, R., Bideau, D., Herbért, R., Niu, Y.L., 1995. Magmatic processes at upper mantle–crustal boundary zone: Garrett transform (EPR South). Journal of Geophysical Research 100, 10,163–10,185.
Hess, H.H., 1962. History of the ocean basins, In: Petrologic Studies: A volume to honour A.F. Buddington, Denver: Geological Society of America, 599–620.
Hofmann, A.W., 1988. Chemical differentiation of the Earth: the relationship between mantle, continental crust, and oceanic crust. Earth and Planetary Science Letters 90, 297–314.
Hofmann, A.W., White, W.M., 1982. Mantle plumes from ancient oceanic crust. Earth and Planetary Science Letters 57, 421–436.
Izbekov, P.E., Eichelberger, J.C., Patino, L.C., Vogel, T.A., Ivanov, B.V., 2002. Calcic cores of plagioclase phenoxcrysts in andessiye from Karymsky volcano: evidence for rapid introduction by basaltic replenishment. Geology 30, 799–802.
Jacobsen, S.B., Wasserburg, G.J., 1979. The mean age of mantle and crustal reservoirs. Journal of Geophysical Research 84, 7411–7427.
Johnson, M.C., Plank, T., 1999. Dehydration and melting experiments constrain the fate of subducted sediments. Geochemistry Geophysics Geosysten 1. 29pp.
Jull, M., Kelemen, P.B., 2001. On the conditions for lower crustal convective stability. Journal of Geophysical Research 106, 6423–6446.
Kay, R.W., Kay, S.M., 1993. Delamination and delamination magmatism. Tectonophysics, 219, 177–189.
Kelemen, P.B., 1995. Genesis of high Mg andesites and the continental crust. Contributions to Mineralogy and Petrology 120, 1–19.
Kelemen, P.B., Hanghoj, K., Greene, A.R., 2003a. One view of the geochemistry of subduction-related magmatic arcs with an emphasis on primitive andesite and lower crust. Treatise on Geochemistry 3, 593–660.
Kelemen, P.B., Yogodzinski, G.M., Scholl, D.W., 2003b. Along-strike variation in lavas of Aleutian island arcs: genesis of high $Mg^{\#}$ andesite and implications for continental crust. Geophysical Monograph 238, 223–276.
Kemp, A.I.S., Hawkesworth, C.J., Paterson, B.A., Kinny, P.D., 2006. Episodic growth of the Gondwana supercontinent from hafnium and oxygen isotopes in zircon. Nature 439, 580–583.
Kerr, A.C., 2003. Oceanic plateaus. Treatise on Geochemistry 3, 537–566.
Klein, E.M., Langmuir, C.H., 1987. Global correlations of ocean ridge basalt chemistry with axial depth and crustal thickness. Journal of Geophysical Research 92, 8089–8115.
Klein, M., Stosch, H.-G., Seck, H.A., 1997. Partitioning of high field-strength and rare-earth elements between amphibole and quartz-dioritic to tonalitic melts: an experimental study. Chemical Geology 138, 257–271.
Klemme, S., Gunther, D., Hametner, K., Prowatke, S., Zack, T., 2006. The partitioning of trace elements between ilmenite, ulvospinel, armalcolite and silicate melts with implications for the early differentiation of the moon. Chemical Geology 234, 251–263.

Kogiso, T., Hirschmann, M.M., 2006. Partial melting experiments of bimineralic eclogite and the role of recycled mafic oceanic crust in the genesis of ocean island basalts. Earth and Planetary Science Letters 249, 188–199.
Kramers, J.D., Tolstikhin, I.N., 1997. Two terrestrial lead isotope paradoxes, forward transport modelling, core formation and the history of the continental crust. Chemical Geology 139, 75–110.
Lambert, I.B., Wyllie, P.J., 1968. Stability of hornblende and a model for the low velocity zone. Nature 219, 1240–1241.
Lambert, I.B., Wyllie, P.J., 1970. Low-velocity zone of the Earth's mantle – incipient melting caused by water. Science 169, 764–766.
Langmuir, C.H., Klein, E.M., Plank, T., 1992. Petrological systematics of mid-ocean ridge basalts: constraints on melt generation beneath ocean ridges. American Geophysical Union Monograph 71, 183–280.
McDonough, W.F., 1990. Constraints on the composition of the continental lithospheric mantle. Earth and Planetary Science Letters 101, 1–18.
McCulloch, M.T., Bennett, V.C., 1994. Progressive growth of the Earth's continental crust and depleted mantle: geochemical constraints. Geochimica et Cosmochimica Acta 58, 4717–4738.
McDonough, W.F., Sun, S.-s., 1995. The composition of the Earth. Chemical Geology 120, 223–253.
Mo, X., Hou, Z., Niu, Y.L., Dong, G., Qu, X., Zhao, Z., Yang, Z., 2007. Mantle contributions to crustal thickening in south Tibet in response to the India–Asia collision. Lithos 96, 225–242.
Mo, X., Niu, Y., Dong, G., Zhao, Z., Hou, Z., Zhou, S., Ke, S., 2008. Contribution of syncollisional felsic magmatism to continental crust growth: a case study of the Paleogene Linzizong Volcanic Succession in southern Tibet. Chemical Geology 250, 49–67.
Nichols, G.T., Wyllie, P.J., Stern, C.R., 1994. Subduction zone melting of pelagic sediments constrained by melting experiments. Nature 371, 785–788.
Nielsen, R.L., Gallahan, W.E., Newberger, F., 1992. Experimentally determined mineral-melt partition coefficients for Sc, Y and REE for olivine, orthopyroxene, pigeonite, magnetite and ilmenite. Contributions to Mineralogy and Petrology 110, 488–499.
Niu, Y.L., 1997. Mantle melting and melt extraction processes beneath ocean ridges: evidence from abyssal peridotites. Journal of Petrology 38, 1047–1074.
Niu, Y.L., 2004. Bulk-rock major and trace element compositions of abyssal peridotites: Implications for mantle melting, melt extraction and post-melting processes beneath ocean ridges. Journal of Petrology 45, 2423–2458 2004.
Niu, Y.L., 2005. Generation and evolution of basaltic magmas: some basic concepts and a hypothesis for the origin of the Mesozoic–Cenozoic volcanism in eastern China. Geological Journal of China Universities 11, 9–46.
Niu, Y.L., 2008. The origin of alkaline lavas. Science 320, 883–884.
Niu, Y.L., Batiza, R., 1994. Magmatic processes at a slow spreading ridge segment: 26°S Mid-Atlantic ridge. Journal of Geophysical Research 99, 19719–19740 1994.
Niu, Y.L., Batiza, R., 1997. Trace element evidence from seamounts for recycled oceanic crust in the eastern Pacific mantle. Earth and Planetary Science Letters 148, 471–483.
Niu, Y.L., Hékinian, R., 1997a. Spreading rate dependence of the extent of mantle melting beneath ocean ridges. Nature 385, 326–329.
Niu, Y.L., Hékinian, R., 1997b. Basaltic liquids and harzburgitic residues in the Garrett Transform: a case study at fast-spreading ridges. Earth and Planetary Science Letters 146, 243–258.
Niu, Y.L., Hékinian, R., 2004. Ridge suction drives plume-ridge interactions (Chapter 9). In: Hékinian, R., Stoffers, P., Cheminée, J.-L. (Eds.), Oceanic Hotspots. Springer-Verlag, New York, pp. 285–307.
Niu, Y.L., O'Hara, M.J., 2003. The origin of ocean island basalts (OIB): a new perspective from petrology, geochemistry and mineral physics considerations. Journal of Geophysical Research 108, 2209. doi:10.1029/2002JB002048. ECV 5-1-19.
Niu, Y.L., O'Hara, M.J., 2008. Global correlations of ocean ridge basalt chemistry with axial depth: a new perspective. Journal of Petrology 49, 633–664.
Niu, Y.L., Lesher, C.M., 1991. Hydrothermal alteration of mafic metavolcanic rocks and genesis of Fe–Zn–Cu sulfide deposits, Stone Hill district, Alabama. Economic Geology 86, 983–1001.
Niu, Y.L., Waggoner, D.G., Sinton, J.M., Mahoney, J.J., 1996. Mantle source heterogeneity and melting processes beneath seafloor spreading centers: the East Pacific Rise, 18° – 19°S. Journal of Geophysical Research 101, 27711–27733.
Niu, Y.L., Collerson, K.D., Batiza, R., Wendt, J.I., Regelous, M., 1999. The origin of E-Type MORB at ridges far from mantle plumes: the East Pacific Rise at 11°20'N. Journal of Geophysical Research 104, 7067–7087.
Niu, Y.L., Bideau, D., Hékinian, R., Batiza, R., 2001. Mantle compositional control on the extent of melting, crust production, gravity anomaly, ridge morphology, and ridge segmentation: a case study at the Mid-Atlantic Ridge 33–35°N. Earth and Planetary Science Letters 186, 383–399.
Niu, Y.L., Regelous, M., Wendt, J.I., Batiza, R., O'Hara, M.J., 2002a. Geochemistry of near-EPR seamounts: importance of source vs. process and the origin of enriched mantle component. Earth and Planetary Science Letters 199, 327–345.
Niu, Y.L., Gilmore, T., Mackie, S., Greig, A., Bach, W., 2002b. Mineral chemistry, whole-rock compositions, and petrogenesis of Leg 176 gabbros: Data and discussion. In: Natland, J.H., Dick, H.J.B., Miller, D.J., Von Herzen, R.P. (Eds.), Proceedings of the Ocean Drilling Program, Scientific Results, vol. 176, pp. 1–60.
Niu, Y.L., O'Hara, M.J., Pearce, J.A., 2003. Initiation of subduction zones as a consequence of lateral compositional buoyancy contrast within the lithosphere: a petrologic perspective. Journal of Petrology 44, 851–866.
Niu, Y.L., Mo, X., Dong, G., Zhao, Z., Hou, Z., Zhou, S., Ke, S., 2007. Continental collision zones are primary sites of net continental crustal growth: Evidence from the Linzizong volcanic succession in southern Tibet. Eos Transactions AGU 88 (52) Fall Meeting, Supplement Abstract V34A-01.
O'Hara, M.J., 1977. Geochemical evolution during fractional crystallization of a periodically refilled magma chamber. Nature 266, 503–507.
O'Hara, M.J., Mathews, R.E., 1981. Geochemical evolution in an advancing, periodically replenished, periodically tapped, continuously fractionating magma chamber. Journal of Geological Society of London 138, 237–277.
O'Hara, M.J., Herzberg, C., 2002. Interpretation of trace element and isotope features of basalts: relevance of field relations, petrology, major element data, phase equilibria, and magma chamber modeling in basalt petrogenesis. Geochimica et Cosmochimica Acta 66, 2167–2191 2002.
O'Nions, R.K., Evensen, N.M., Hamilton, P.J., 1979. Geochemical modeling of mantle differentiation and crustal growth. Journal of Geophysical Research 84, 6091–6101.
O'Reilly, Y.S., Griffin, W.L., 1988. Mantle metasomatism beneath western Victoria, Australia: I, Metasomatic processes in Cr-diopside lherzolites. Geochimimica et Cosmochimica Acta 52, 433–447.
Pan, G.T., Ding, J., Yao, D.S., Wang, L.Q., 2004. Guidebook of 1: 1, 500, 000 geologic map of the Qinghai-Xizang (Tibetan) plateau and adjacent areas. Chengdu Cartographic Publishing House, China. 48 pp.
Parman, S.W., 2007. Helium isotopic evidence for episodic mantle melting and crustal growth. Nature 446, 900–903.
Pearcy, J.G., DeBari, S.M., Slep, N.H., 1990. Mass balance calculations for two sections of island arc crust and implications for the formation of continents. Earth and Planetary Science Letts 96, 427–442.
Pearson, D.G., Nowell, G.M., 2002. The continental lithospheric mantle: characteristics and significance as a mantle reservoir. Philosophical Transaction, Royal Society A360, 2383–2410.
Pearson, D.G., Parman, S.W., Nowell, G.M., 2007. A link between large mantle melting events and continent growth seen in osmium isotopes. Nature 449, 202–205.
Phipps Morgan, J., 1987. Melt migration beneath mid-ocean ridge spreading centers. Geophysical Research Letters 14, 1238–1241.
Phipps Morgan, J., Morgan, W.J., Zhang, Y.-S., Smith, W.H.F., 1995. Observational hints for a plume-fed, suboceanic asthenosphere and its role in mantle convection. Journal of Geophysical Research 100, 12,753–12,767.
Pietranik, A., Koepke, J., Puziewicz, J., 2006. Crystallization and resorption in plutonic plagioclase: implications on the evolution of granodiorite magma (Ge˛siniec granodiorite, Strzelin Crystalline Massif, SW Poland). Lithos 86, 260–280.
Pilet, S., Baker, M.B., Stolper, E.M., 2008. Metasomatized lithosphere and the origin of alkaline lavas. Science 320, 916–919.
Plank, T., 2005. Constraints from Thorium/Lanthanum on sediment recycling at subduction zones and the evolution of continents. Journal of Petrology 46, 921–944.
Plank, T., Langmuir, C.H., 1998. The chemical compositions of subducting sediments and its consequences for the crust and mantle. Chemical Geology 145, 325–394.
Polat, A., Kerrich, R., Wyman, D.A., 1998. The late Archean Schreiber-Hemlo and White River-Dayohessarah greenstone belts, Superior Province: collages of oceanic plateaus, ocean arcs, and subduction-accretion complexes. Tectonophysics 289, 295–326.
Rapp, R.P., 1995. Amphibolite-out phase boundary in partially melted metabasalt, its control over liquid fraction and composition, and source permeability. Journal of Geophysical Research 100, 15601–15610.
Rapp, R.P., Watson, E.B., 1995. Dehydration melting of metabasalt at 8–32 kbar: Implications for continental growth and crust–mantle recycling. Journal of Petrology 36, 891–931.
Prytulak, J., Elliott, T., 2007. TiO_2 enrichment in ocean island basalts. Earth Planetary Science Letters, 263, 388–403.
Regelous, M., Niu, Y.L., Wendt, J.I., Batiza, R., Greig, A., Collerson, K.D., 1999. An 800 Ka record of the geochemistry of magmatism on the East Pacific Rise at 10°30'N: insights into magma chamber processes beneath a fast-spreading ocean ridge. Earth and Planetary Science Letters 168, 45–63 1999.
Regelous, M., Niu, Y.L., Abouchami, W., Castillo, P.R., 2009. Shallow origin for South Atlantic Dupal Anomaly from lower continental crust: Geochemical evidence from the Mid-Atlantic Ridge at 26°S. Lithos 112, 57–72 (this issue).
Ren, M., Parker, D.F., White, J.C., 2003. American Mineralogist 88, 1091–1103.
Rudnick, R.L., 1992. Restite, Eu anomalies, and the lower continental crust. Geochimica et Cosmochimica Acta 56, 963–970.
Rudnick, R.L., 1995. Making continental crust. Nature 378, 571–578.
Rudnick, R.L., Fountain, D.M., 1995. Nature and composition of the continental crust: a lower crustal perspective. Review of Geophysics 33, 267–309.
Rudnick, R.L., Gao, S., 2003. Composition of the continental crust. Treatise on Geochemistry 3, 1–64.
Saal, A.E., Kurz, M.D., Hart, S.R., Blusztajn, J.S., Blichert-Toft, J., Liang, Y., Geist, D.J., 2007. The role of lithospheric gabbros on the composition of Galapagos lavas. Earth and Planetary Science Letters 257, 391–406.
Scholl, D.W., von Huene, R., 2004. Recycling of continental crust at ocean margin subduction zones: evidence and implications for the growth of continental crust and supercontinent reconstruction. Presentation at "Plate Tectonic, Plumes and Planetary Lithospheres Conference – Celebration of Kevin Burke's 75th Birthday", Houston, November 12–15, 2004.
Shannon, R.D., 1976. Revised effective radii and systematic studies of interatomic distance in halides and chalcogenides. Acta Crystallographica A32, 751–767.
Sobolev, A.V., Hofmann, A.W., Nikogosian, I.K., 2000. Recycled oceanic crust observed in "ghost plagioclase" within the source of Mauna Loa lavas. Nature 404, 986–990.
Sobolev, A.V., Hofmann, A.W., Kuzmin, D.V., et al., 2007. The amount of recycled crust in sources of mantle derived melts. Science 316, 412–417.
Staudigel, H., 2003. Hydrothermal alteration processes in the oceanic crust. Treatise on Geochemistry 3, 511–535.
Stein, M., Hofmann, A.W., 1994. Mantle plumes and episodic crustal growth. Nature 372, 63–68.
Stein, C.A., Stein, S., 1992. A model for the global variation in oceanic depth and heat flow with lithospheric age. Nature 359, 123–129.

Stern, C.R., Huang, W.L., Wyllie, P.J., 1975. Basalt-andesite-rhyolite-H_2O: crystallization intervals with excess H_2O and H_2O-undersaturated liquidus surfaces to 35 kilobars, with implications for magma genesis. Earth and Planetary Science Letters 28, 189–196.
Sun, C.-O., Williams, R.J., Sun, S.-S., 1974. Distribution coefficients of Eu and Sr for plagioclase-liquid and clinopyroxene-liquid equilibria in oceanic ridge basalt: an experimental study. Geochimica et Cosmochimica Acta 33, 1415–1433.
Sun, S.-s., McDonough, W.F., 1989. Chemical and isotopic systematics of ocean basalt: Implications for mantle composition and processes. Geological Society Special Publication 42, 323–345.
Takahashi, N., Kodaira, S., Klemperer, L.S., Tatsumi, Y., Kaneda, Y., Suyehiro, K., 2007. Crustal structure and evolution of the Mariana intra-oceanic island arc. Geology 35, 203–206.
Tatsumi, Y., 2006. High-Mg andesites in the Setouchi volcanic belt, Southwestern Japan: analogy to Archean magmatism and continental crust formation? Annual Review of Earth and Planetary Sciences 34, 467–499.
Taylor, S.R., 1967. The origin and growth of continents. Tectonophysics 4, 17–34.
Taylor, S.R., 1977. Island arc models and the composition of the continental crust. In: Talwani, M., PitmanIII III, W.C. (Eds.), Island Arcs, Deep Sea Trenches, and Back-Arc Basins. Maurice Ewing Series, vol. 1. AGU (American Geophysical Union), Washington, D.C., pp. 325–335.
Taylor, S.R., McLennan, S.M., 1985. The continental crust: Its composition and evolution. Blackwell, Oxford. 312 pp.
Taylor, S.R., McLennan, S.M., 1995. The geochemical evolution of the continental crust. Review of Geophysics 33, 241–265.
Tiepolo, M., Vannucci, R., Oberti, R., Foley, S., Bottazzi, P., Zanetti, A., 2000. Nb and Ta incorporation and fractionation in titanian pargasite and kaersutite: crystal-chemical constraints and implications for natural systems. Earth and Planetary Science Letters 176, 185–201.
van der Hilst, R.D., Widiyantoro, S., Engdahl, E.R., 1997. Evidence for deep mantle circulation from global tomography. Nature 386, 578–584.
von Huene, Scholl, D.W., 1991. Observations at convergent margins concerning sediment subduction, subduction erosion, and the growth of continental crust. Review of Geophysics 29, 279–316.
Wedepohl, H., 1995. The composition of the continental crust. Geochimica et Cosmochimica Acta 59, 1217–1239.
Wendt, J.I., Regelous, M., Niu, Y.L., Hékinian, R., Collerson, K.D., 1999. Geochemistry of lavas from the Garrett Transform Fault: insights into mantle heterogeneity beneath the eastern Pacific. Earth and Planetary Science Letters 173, 271–284.
White, R.S., McKenzie, D.P., O'Nions, R.K., 1992. Oceanic crustal thickness from seismic measurements and rare earth elements inversions. Journal of Geophysical Research 97, 19683–19715.
Wolf, M.B., Wyllie, P.J., 1994. Dehydration melting of amphibolite at 10 kbar: effects of temperature and time. Contributions to Mineralogy and Petrology 115, 369–383.
Workman, R.K., Hart, S.R., 2005. Major and trace element composition of depleted MORB mantle (DMM). Earth and Planetary Science Letters 231, 53–72.
Wyllie, P.J., Wolfe, M.B., 1993. Dehydration-melting of amphibolite: sorting out the solidus. Geological Society Special Publication 76, 405–416.
Zindler, A., Hart, S.R., 1986. Chemical geodynamics. Annual Review of Earth and Planetary Sciences 14, 493–571.
Zindler, A., Staudigel, H., Batiza, R., 1984. Isotope and trace element geochemistry of young Pacific seamounts: implications for the scale of upper mantle heterogeneity. Earth and Planetary Science Letters 70, 175–195.